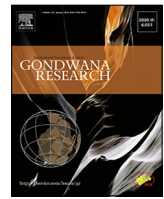




ELSEVIER

Contents lists available at ScienceDirect

## Gondwana Research

journal homepage: [www.elsevier.com/locate/gr](http://www.elsevier.com/locate/gr)

## GR Focus Review

## Terrestrial records of weathering indicate three billion years of dynamic equilibrium



Rebecca M. Dzombak, Nathan D. Sheldon \*

Dept. of Earth and Environmental Sciences, University of Michigan, United States

## ARTICLE INFO

## Article history:

Received 13 December 2021

Revised 22 April 2022

Accepted 12 May 2022

Available online 18 May 2022

Handling Editor: A. Festa

## Keywords:

Paleosols

Weathering

Terrestrial geochemistry

Carbon cycle

## ABSTRACT

Although continental weathering intensity has been invoked as a primary control on biogeochemistry, tectonics, and the carbon cycle throughout geologic history, it remains poorly quantified over Earth's history. As a direct product of continental weathering, paleosols (fossil soils) offer unique insight into past weathering intensity, but they remain underused in efforts to constrain terrestrial weathering patterns over geologic time. Here, we compile the largest terrestrial weathering record to date, comprising 248 paleosol and weathering profiles that span three billion years. We analyze a suite of weathering indices to test common hypotheses around state-changes in terrestrial weathering intensity due to atmospheric changes and terrestrial biosphere expansion. Contrary to commonly invoked assumptions, we find that these weathering indices reflect consistent average terrestrial weathering intensity through time. No unidirectional state changes in average weathering intensity, as have previously been hypothesized, are detectable in the record. However, Phanerozoic paleosols preserve an increase in the total range of Chemical Index of Alteration (CIA) values, with the increased CIA range driven by the appearance of high-CaO paleosols. We compare the paleosol weathering record to weathering intensities recorded by select fluvial sandstones and diamictites.

We interpret the overall stability of the continental weathering record as reflecting the baseline level of weathering from which the Earth system deviates during periods of perturbation (i.e., major climate transitions, rapid tectonic activity). With consistent weathering intensity over geologic timescales, the record supports subaerially-emerged continental area as a critical control on total potential erosional flux and nutrient flux to the oceans. The paleosol community should work to build an even more complete database of paleosol geochemistry to allow more nuanced analyses of terrestrial weathering through time.

© 2022 International Association for Gondwana Research. Published by Elsevier B.V. All rights reserved.

## Contents

1. Introduction . . . . .	377
1.1. Continental weathering, erosion, and biogeochemical transitions through time . . . . .	378
1.2. Quantifying continental weathering . . . . .	379
2. Methods . . . . .	379
2.1. Paleosol compilation and screening, and other data collection . . . . .	379
2.2. Geochemical indices . . . . .	380
2.3. Data distributions and bootstrap analyses . . . . .	382
3. Results . . . . .	382
3.1. Weathering through time . . . . .	382
3.2. Distribution of soil orders through time . . . . .	383
4. Discussion . . . . .	383
4.1. What does a stable weathering paleosol record mean? . . . . .	383
4.2. Timescales of weathering intensity events and the geologic baseline . . . . .	386
4.3. Changes in dominant weathering mechanisms over time . . . . .	386

\* Corresponding author at: 1100 N. University Ave, Ann Arbor, MI 48109, United States.

E-mail address: [nsheldon@umich.edu](mailto:nsheldon@umich.edu) (N.D. Sheldon).

4.4.	Distribution through time and biases in the paleosol record . . . . .	387
4.4.1.	Weathering profile and paleosol thickness through time . . . . .	387
4.4.2.	Paleosol bias and climate . . . . .	387
4.4.3.	Paleosol bias from the biosphere . . . . .	387
4.4.4.	Geomorphologic evolution and soil order through time . . . . .	388
4.4.5.	Weathering in LIPs and volcanic arcs . . . . .	388
4.4.6.	Sampling biases in paleosol research . . . . .	389
4.5.	Implications for reconstructing past climates and biogeochemical cycling . . . . .	389
4.6.	Next steps . . . . .	389
5.	Conclusions . . . . .	389
	Declaration of Competing Interest . . . . .	390
	Acknowledgments . . . . .	390
	Appendix A. Supplementary material . . . . .	390
	References . . . . .	390

## 1. Introduction

Subaerial weathering of continents has been invoked as both a cause and consequence of multiple major biogeochemical transitions throughout geologic time, as outlined below (see Figs. 1 and 2b for periods of interest). However, how the intensity and style of weathering changed remains poorly understood due to a relative dearth of direct evidence. Marine sediment geochemical records can reflect terrestrial weathering (e.g., Fedo et al., 1996; Blum et al., 1998; Bahlburg and Dobrzinski, 2011; von Strandmann et al., 2021) and provide useful proxies for the timing and magnitude of continental weathering and erosion, but as the sediment sink, they are limited in their ability to reflect surface conditions directly. Marine records containing terrigenous sediments are also affected by (bio)geochemical processes in the water

column that can, in turn, be affected by rates of continental weathering and erosional fluxes. Disentangling terrestrial signals from marine water column geochemistry, as well as from post-depositional alteration signals, is crucial for understanding the co-evolution of the terrestrial geosphere, marine biosphere, and the atmosphere. To help clarify the terrestrial weathering signal through time, continental weathering intensity can be directly quantified using the rock record of *in situ* weathering products (i.e., paleosols and weathering profiles), and more indirectly through fluvial sandstones which, like detrital shales and marine basin drainage formations records (e.g., Hessler et al., 2017), can record a basin-wide weathering intensity signal. Finally, improving understanding of the terrestrial weathering on Earth may improve our ability to accurately and confidently interpret similar types of weathering records on Mars.

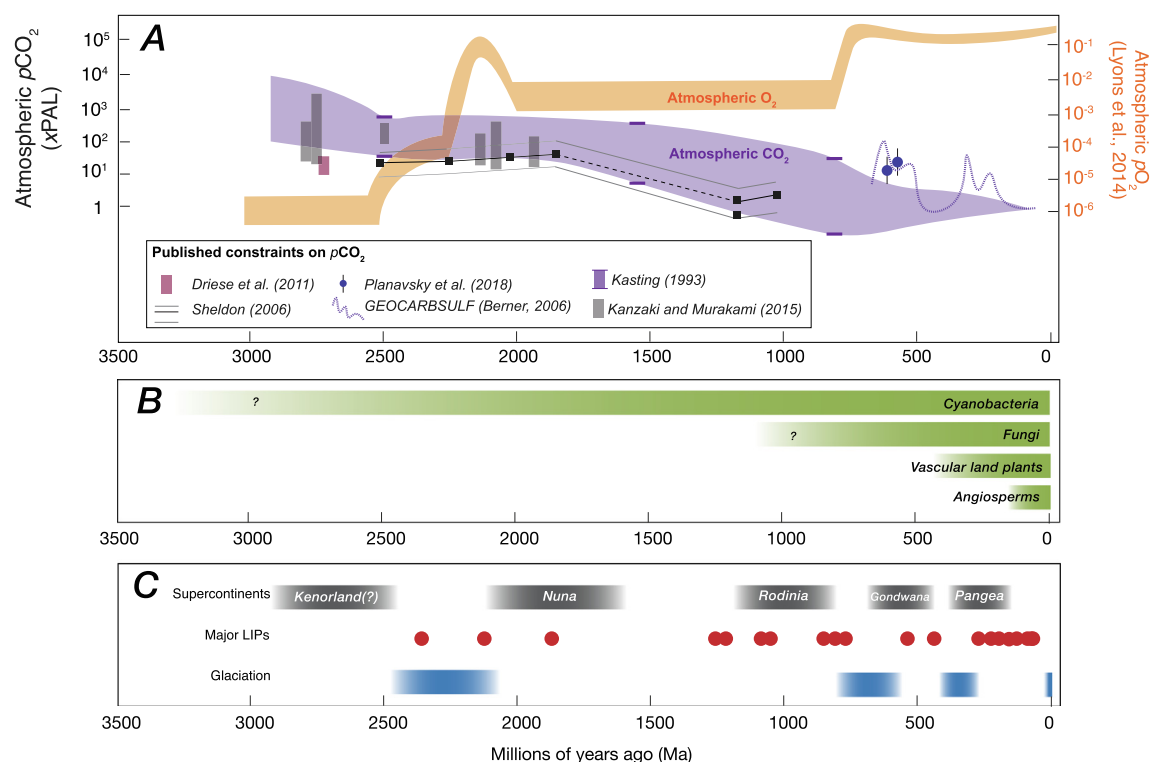


**Fig. 1.** (A) Generalized evolution of atmospheric composition, with  $pCO_2$  from multiple sources (Kasting, 1993; Berner, 2006; Sheldon, 2006a,b; Driese et al., 2011; Kanzaki and Murakami, 2015; Planavsky et al., 2018) and  $pO_2$  in orange (Lyons et al., 2014). Modified from Sheldon et al. (2021). (B) Major terrestrial biological innovations relevant to continental weathering and pedogenesis through time. (C) Generalized climatic and tectonic contexts to consider as factors for weathering intensity through time. Gray bars are approximate durations of supercontinents (Domeier et al., 2018; Pastor-Galán et al., 2019), red dots are LIPs with erupted volumes  $> 1 \text{ Mm}^3$  (Ernst et al., 2021), and blue bars approximate the duration of major glaciations.

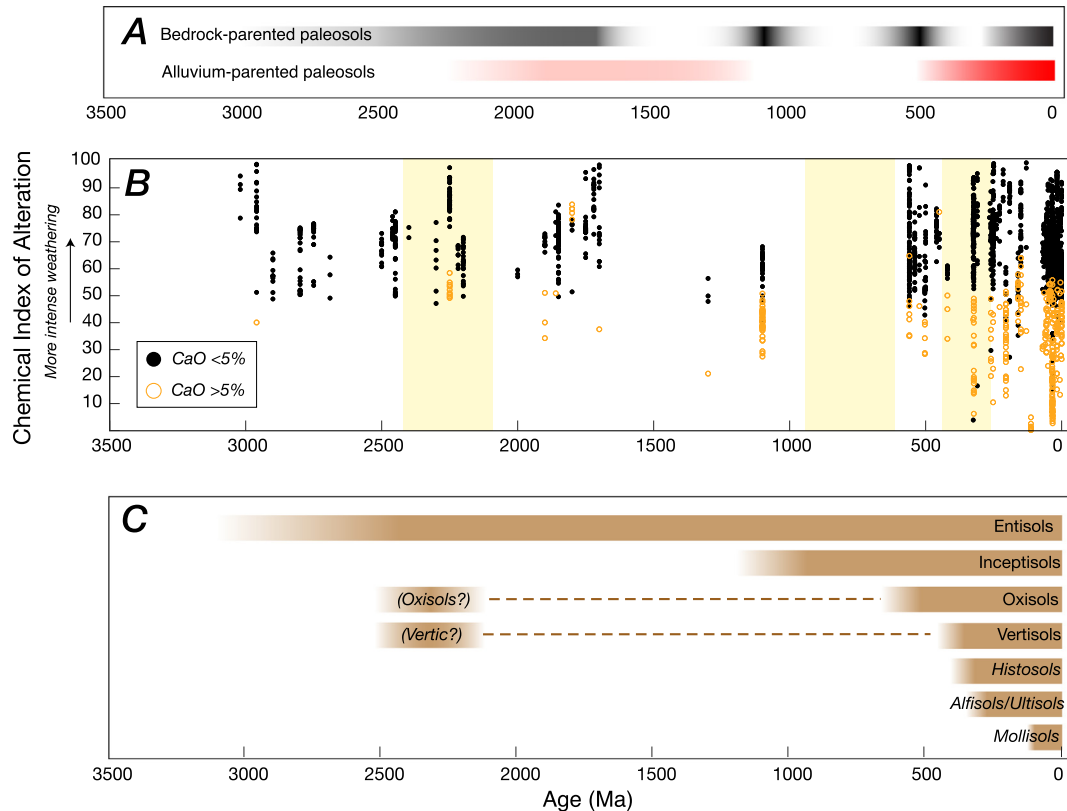


**Fig. 2.** (A) Cartoon representation of the general distribution of paleosols and weathering profiles included in this dataset through time. (B) CIA in paleosols and weathering profiles (individual samples) through time, with samples with CaO > 5 % marked by hollow orange circles (Sheldon et al., 2002; Prochnow et al., 2006). Sandstones are excluded from this plot. General periods where changes in continental weathering intensity have been posited are highlighted in yellow (i.e., the Great Oxygenation Event, Neoproterozoic glaciations, and the evolution of the terrestrial biosphere). (C) Semi-quantitative schematic depicting the appearance of soil orders (as defined by modern USDA soil taxonomy) in geologic time (based on Retallack 2001). Soil order names in italics have few samples in the present compilation, so their appearances are inferred based on known terrestrial biosphere evolutions. Soil order names in italics and parentheses (*Vertic?*) represents a designation made in the literature that remains debated. Only soil orders commonly found in the rock record are included.

### 1.1. Continental weathering, erosion, and biogeochemical transitions through time

Continently derived sediments are the main source of nutrients (e.g., P, Fe) for the marine biosphere, and several key biogeochemical transitions in Earth's history have been linked to changes in the intensity and magnitude of continental weathering. Continental weathering would have begun when continents first emerged and were permanently exposed to the atmosphere between ca. 3.3–2.5 Ga (billion years) ago (see Korenaga 2018 and refs. therein; Buick et al., 1995; Chowdhury et al., 2021; Wang et al., 2021). As atmospheric oxygen increased during the Neoarchean and Paleoproterozoic (Fig. 1a), the dominant weathering regime shifted from abiotic CO<sub>2</sub> acid weathering to both oxidative and acid weathering (e.g., Anbar et al., 2007; Reinhard et al., 2009; Kendall et al., 2015; Somelar et al., 2020; Lipp et al., 2021; Sheldon et al., 2021; Sheldon, 2013). Throughout the Proterozoic, continental weathering-derived fluxes (e.g., C, Fe, P) from the continents are thought to have contributed to changing ocean chemistry and shifted nutrient limitation (e.g., Anbar and Knoll, 2002; Berner, 2004; Lenton and Watson, 2004; Mills et al., 2011; Sahoo et al., 2012; Lyons et al., 2014; Cermeño et al., 2015; Laakso et al., 2020).

Continental weathering during the Neoproterozoic has been invoked as a driver of several critical biological and geochemical changes in Earth's history, including the rise of atmospheric oxygen and the evolution of animal life (e.g., Donnadieu et al., 2004;

Lenton and Watson, 2004; Halverson et al., 2009). The Neoproterozoic saw global glaciations, the formation and breakup of supercontinents, and potential oscillations in atmospheric composition (Carver and Vardavas, 1994; see Och and Shields-Zhou, 2012 for review), all of which can be tied to weathering, erosion, and terrestrial-to-marine nutrient fluxes. In particular, weathering-driven fluxes of P have been hypothesized as a control on marine productivity, oxygenation, climate, and atmospheric composition (Donnadieu et al., 2004; Campbell and Squire, 2010; Planavsky et al., 2010; Mills et al., 2011; Och and Shields-Zhou, 2012; Brocks et al., 2017; Reinhard et al., 2017; Reinhard et al., 2020). But constraining that critical P flux depends, in part, on quantifying terrestrial weathering, the style of which may have changed dramatically in the early Phanerozoic with the rise of rooting terrestrial vegetation.

The evolution of rooting by vascular land plants in the Devonian (Fig. 1b) and a resulting change in weathering intensity has been hypothesized as a driver of change in oxygenation and climate, ultimately culminating in the late Paleozoic ice age (e.g., Algeo et al., 1995; Algeo and Scheckler, 1998; Berner, 1998; Lenton, 2001; Lenton and Watson, 2004; Porada et al., 2016; D'Antonio et al., 2020; Davies et al., 2021). Additionally, changes in fluvial geomorphology resulting from rooting by land plants and consequent shifts in sediment supply could have influenced erosional fluxes beginning around this time (e.g., Davies and Gibling, 2010; Davies et al., 2021; see Algeo et al., 1995, Gurnell, 2013, Pawlik et al., 2020, and Ielpi et al., 2022 for reviews).

In the Cenozoic, links between the rate of continental silicate weathering and a cooling climate have been proposed, but whether weathering causes cooling or vice versa remains debated (e.g., Molnar and England, 1990; Raymo and Ruddiman, 1992; Willenbring and von Blanckenburg, 2010; Caves et al., 2016). Links between Cenozoic erosion and marine productivity have also been proposed (e.g., Cermeño et al., 2015). Finally, the emplacement of large igneous provinces (LIPs; Fig. 1c) and formation of volcanic arcs have been invoked as drivers for weathering rate increases and climate changes via  $\text{CO}_2$  release versus drawdown (e.g., Cohen and Coe, 2002; Lee et al., 2015; Cox et al., 2016; Sternai et al., 2019; Park et al., 2020; Gernon et al., 2021; Longman et al., 2022) because they represent relatively large pools of easily weatherable materials (e.g., Dessert et al., 2003); however, more data are needed to quantify the relationship between these events, soil formation, and global average weathering intensity. Despite the central role continental weathering plays in many fundamental questions around climate, tectonics, and the biosphere, weathering intensity through time remains poorly understood, with an imbalance of data and analysis between the sources (i.e., paleosols, terrestrial sediments) and sinks (i.e., shales, from which the source is commonly inferred).

## 1.2. Quantifying continental weathering

Efforts to constrain and quantify continental weathering through time have typically focused on several tools: mass-balance and kinetic modeling approaches based on sedimentology, mineralogy, and atmospheric composition (e.g., Francois and Walker, 1992; Rye and Holland, 1998; Murakami et al., 2004; Berner, 2006; Fabre et al., 2011; Lyons et al., 2014; Kendall et al., 2015; Hao et al., 2017, 2020); Sr and Nd isotopes (e.g., Brass, 1975; Martin and Macdougall, 1995; Blum et al., 1998; Theiling et al., 2012; Bayon et al., 2021); weathering indices such as CIA and clay mineralogy in shale and glacial records (Kelly et al., 2005; Fedo et al., 1996; Bahlburg and Dobrzinski, 2011; Gaschnig et al., 2014; Lipp et al., 2021; von Strandmann et al., 2021); and most recently, efforts using large community-built datasets such as MacroStrat and the Sedimentary Geochemistry and Paleoenvironments Project (Peters et al., 2018; Farrell et al., 2021; Lipp et al., 2021). The growing use of community databases of terrestrial geochemistry is an exciting step for the field, but paleosols and weathering profiles with elemental rather than only isotopic data struggle to hold attention due to their low numbers compared to other terrestrial sediment types. Despite their relatively small contribution to the overall rock record, paleosols' weathering intensities are worth studying.

Paleosols offer a unique, direct record of climatic, biologic, and atmospheric conditions at Earth's surface as soils were being formed. They have been used in a relatively limited sense to address weathering through geologic time, with work typically focusing on a small suite of elements of interest (e.g., Colwyn et al., 2019), individual paleosol profiles as case studies for areas or environments of interest, or a high-resolution basin-scale records of paleosols through geologically short periods of time (e.g., Bestland et al., 1997; Sheldon et al., 2002; Kraus and Riggins, 2007; Hyland et al., 2017). Compilations of longer records (billions of years) have been limited to a small number (ca. 15 profiles) of very well-studied, primarily bedrock-parented profiles through time (e.g., Rye and Holland, 1998; Sheldon, 2006a,b; Colwyn et al., 2019; Beaty and Planavsky, 2021). This approach offers a thoroughly vetted but ultimately skeletal view of continental weathering through time. To understand links between continental weathering and global biogeochemical changes through geologic time, a higher-resolution record that extends beyond only the handful of intensely studied profiles is necessary.

Here, we compile the largest ca. 3-billion-year record of weathering intensity in paleosols and use it to test hypothesized changes in weathering intensity, as well as to explore the nature of pedogenesis through geologic history. We build such a dataset by including select other bedrock-parented weathering profiles and alluvium-parented paleosols, which can be compared to underlying sediments and can undergo similar, if not identical, quality-control checks (i.e., establishing reasonable parent material, avoiding diagenetically-influenced profiles, only including profiles with multiple samples) as bedrock-parented paleosols. Alluvium-parented paleosols are frequently used for paleoclimatic and paleoenvironmental reconstructions and are considered viable recorders of at least regional weathering intensity; therefore, we include them here.

As a point of context and comparison, we also gathered geochemical data from select fluvial deposits (i.e., sandstones, siltstones, mudstones) through time. While the accumulation of a fluvial deposit is inherently a different process from soil formation, we opted to include these because they ultimately reflect a snapshot of watershed-wide weathering intensity in a manner comparable to detrital shales serve. Fluvial networks are the transport mechanism between the source and sink, so it is worthwhile to examine them for any secular evolution as well. Fluvial deposits also depend upon, to some degree, the composition of the watershed's soils. Finally, we were interested to see how well the global weathering intensity the fluvial deposits matched that of global paleosols for a given time; a potential positive outcome of such an analysis could be determining what sedimentary records can best be used to infer continental weathering when paleosols are absent. To this end, we also compared to the weathering intensity of glacial diamictites over time, in part because they are the only record of terrestrial weathering processes during the "snowball Earth" events. This expanded record provides critical new constraints for the terrestrial sediment supply as a counterpart to the well-studied marine weathering sink represented by shales.

With this compilation, we can begin to address some of the outstanding questions in weathering and biogeochemistry mentioned above. Specifically, we address the following questions: Do paleosols record state changes in weathering intensity at key points (i.e., rise of oxygen, the Neoproterozoic, land plant evolution) over the past 3 billion years, as have been hypothesized? And how does the paleosol record reflect changes in soil-forming processes through time?

## 2. Methods

We collected bulk oxide geochemical data and descriptive information for paleosols and weathering profiles (n profiles = 248; bedrock-parented = 85, alluvium-parented = 138, sandstones/mud stones = 25; Fig. 1a, Supplemental Table 1) from the literature following the methods below. There are thousands of stable isotopic analyses of paleosols in the literature for used paleoaltimetry or paleohydrological reconstructions (e.g., compilations in Sheldon and Tabor, 2009; Jolivet and Boulvais, 2021); however, most of those studies lack other elemental data essential for calculating weathering intensity, so we have not included isotope-only studies in our compilation. A complete list of the studies and samples, and their geochemical data, contained in the following analyses can be found in Supplemental Table 1.

### 2.1. Paleosol compilation and screening, and other data collection

We included a range of parent materials (bedrock and alluvial) to capture as much variability as possible in the weathering products (Fig. 1a). To be included as bedrock-parented profile, paleosols

or weathering profiles had to adhere the criteria outlined by [Rye and Holland \(1998\)](#). These are:

1. Homogenous parent material and preserved in-place;
2. Up-profile changes in mineralogy,
3. in texture, and
4. in chemical composition that follow soil weathering profiles; and
5. For Precambrian profiles, either soft-sediment deformation between the top of the paleosol and overlying rocks or the presence of corestones/rip-up clasts

It should be noted that preserving the true tops of paleosols, particularly compound/composite paleosols (e.g., [Kraus, 1999](#)) that become more common in the Phanerozoic, is relatively rare. While most of the profiles used in this work feature corestones or rip-up clasts at their base, fewer have the full profile preserved, particularly in Phanerozoic soils which tended to have erosive tops. In cases where profile tops were eroded but the profile was confidently a paleosol and fit the other four criteria, profiles were included. Profile tops (i.e., O and A horizons in modern soils) are further from long-term equilibrium with the climate and atmosphere than lower regions in a profile (i.e., B horizons, used for weathering indices) because they may be subject to short-term environmental perturbations that do not affect the deeper parts of the soil profiles. Alluvium-parented paleosols were judged on as many of these criteria as applicable and were only included if mineralogy, textures, and chemical compositions suggestive of pedogenesis, along with pedogenic features (e.g., root traces, reduction mottles, slickensides, ped structures) were present.

The focus of this work was on the paleosol-parent comparison, in part because of difficulties in confidently designating paleosol horizons in the early Phanerozoic or prior, or where horizons were simply not reported. In averaging the weathered profile or paleosol, we considered horizons above BC to be the paleosol where such designations were provided. For Precambrian weathering profiles where modern horizonation does not apply, the profile was considered weathered up to corestones and/or weathered bedrock (reporting style and quality varies through time). For certain Precambrian weathering profiles, mineral zones by depth were used to differentiate weathering profile from bedrock (e.g., sericite zones over bedrock). When possible, we compared those zones to geochemical down-profile trends (e.g., CIA, Al, or Ti) as an additional quality check. This “lumping” approach aids in avoiding issues of defining horizons and orders, which are not typically applicable in early Phanerozoic soils and prior.

Not all sedimentary beds called paleosols in the literature were included, particularly during the Precambrian. Known disputed paleosols (e.g., where one worker has identified a paleosol and another a turbidite) were excluded.

For all profile types, we excluded profiles above greenschist-grade metamorphism because of the potential for hydrothermal alteration and loss of original weathering intensity signals and excluded any profiles with significant potassium metasomatism or hydrothermal alteration. When building future versions of this dataset, workers could employ the [Fedø et al. \(1995\)](#) approach to correct for metasomatism, potentially expanding the number of Precambrian profiles included. Additionally, we checked for post-pedogenic addition of material using down-profile Ti/Al and excluded any profiles with apparent material addition (i.e., variability in Ti/Al between bedrock and overlying weathering profile/paleosol; see [Sheldon and Tabor, 2009](#)).

We collected or estimated soil and weathering profile thicknesses as available (Supplemental Table 2). Profile thickness was taken from the uppermost horizon or part of the profile to parent rock or the appearance of corestones (individual pieces of parent

material above the massive parent material surface). We noted soil orders when available, but due to sample size limitations and sampling bias (i.e., certain orders tend to be both more commonly found and more frequently sampled, such as Vertisols), we only consider soil order data in a qualitative sense. Only paleosols were included in the analyses of weathering intensity through time; values from fluvial and glacial sediments serve only as points of comparison and context.

As the middle step between soil formation and deposition in marine basins, large fluvial sandstones are a natural complement to paleosol geochemical record. To represent larger known catchments of terrestrial weathering during periods when paleosols were scarce (e.g., Jacobsville Sandstone, ca. 960 Ma–1.1 Ga, [Malone et al., 2016](#)), we included select massive fluvial sandstones and undifferentiated mudstones. We consider that these are appropriate to include because while paleosols represent *in situ* weathering intensity, these large-scale fluvial sandstones represent the mixed weathered product of a watershed that was being eroded and ultimately transported to the oceans, albeit biased toward sand- and silt-sized fractions of the bedload. (A point worthy of consideration, as the clay-sized fraction could be more likely to record a more intense weathering signal and is likely to be transported further in the source-sink pathway; quantifying such a bias would be valuable in quantifying baseline weathering intensities for the source, transport, and sink.) If sandstones incorporate reworked or eroded soil material, for the purposes here, this can be viewed as essentially contemporaneous terrestrial weathering signals from the same basin, fulfilling the purpose of this work. We recognize factors other than bedrock, soil chemistry, and weathering intensity influence fluvial sediment geochemistry; however, particulate geochemistry and bedload composition could be more difficult to alter than dissolved-load geochemistry, so we posit that it is at least somewhat representative of the watershed. Future work could explore this potential further by comparing soil geochemistry, various fluvial deposits and intraclasts, and sink sediments, capturing a complete, basin-wide picture of weathering signals.

Similarly, glacially-derived sediments (i.e., tillites, diamictites) can provide a point of comparison for terrestrial weathering records during glacial periods when paleosols may be less likely to be formed and/or preserved. We include a weathering record from tillites through time ([Fig. 6; Gaschnig et al., 2014](#)) to fill in gaps in the terrestrial weathering record from paleosols. Together, these records ([Fig. 1](#)) create an interconnected picture of terrestrial weathering for the past three billion years.

## 2.2. Geochemical indices

Geochemical analyses for this work focused on established weathering indices: the Chemical Index of Alteration (CIA; [Nesbitt and Young, 1982](#)), CIA without potash (CIA-K; [Maynard, 1992](#)), and oxic and reducing Mafic Index of Alteration (MIA<sub>ox,red</sub>; [Babechuk et al., 2014](#)). Equations for each of these indices are below, with possible values ranging from 0 to 100 (low to high weathering intensity) for both CIA(-K) and MIA<sub>ox,red</sub>. CIA and CIA-K reflect plagioclase weathering, where the latter excludes K to account for K metasomatism ([Maynard, 1992](#)). MIA was developed to reflect weathering of mafic substrates (e.g., basalt, a common parent material through time; [Babechuk et al., 2014](#)) and includes Fe and Mg, which are common in high-temperature silicates in mafic rocks. By comparing patterns in these indices through time, we can see if pedogenic processes vary in intensity.

$$\text{CIA} = \text{Al}_2\text{O}_3 / (\text{Al}_2\text{O}_3 + \text{CaO} + \text{Na}_2\text{O} + \text{K}_2\text{O}) * 100 \quad (1)$$

$$\text{CIA-K} = \text{Al}_2\text{O}_3 / (\text{Al}_2\text{O}_3 + \text{CaO} + \text{Na}_2\text{O}) * 100 \quad (2)$$

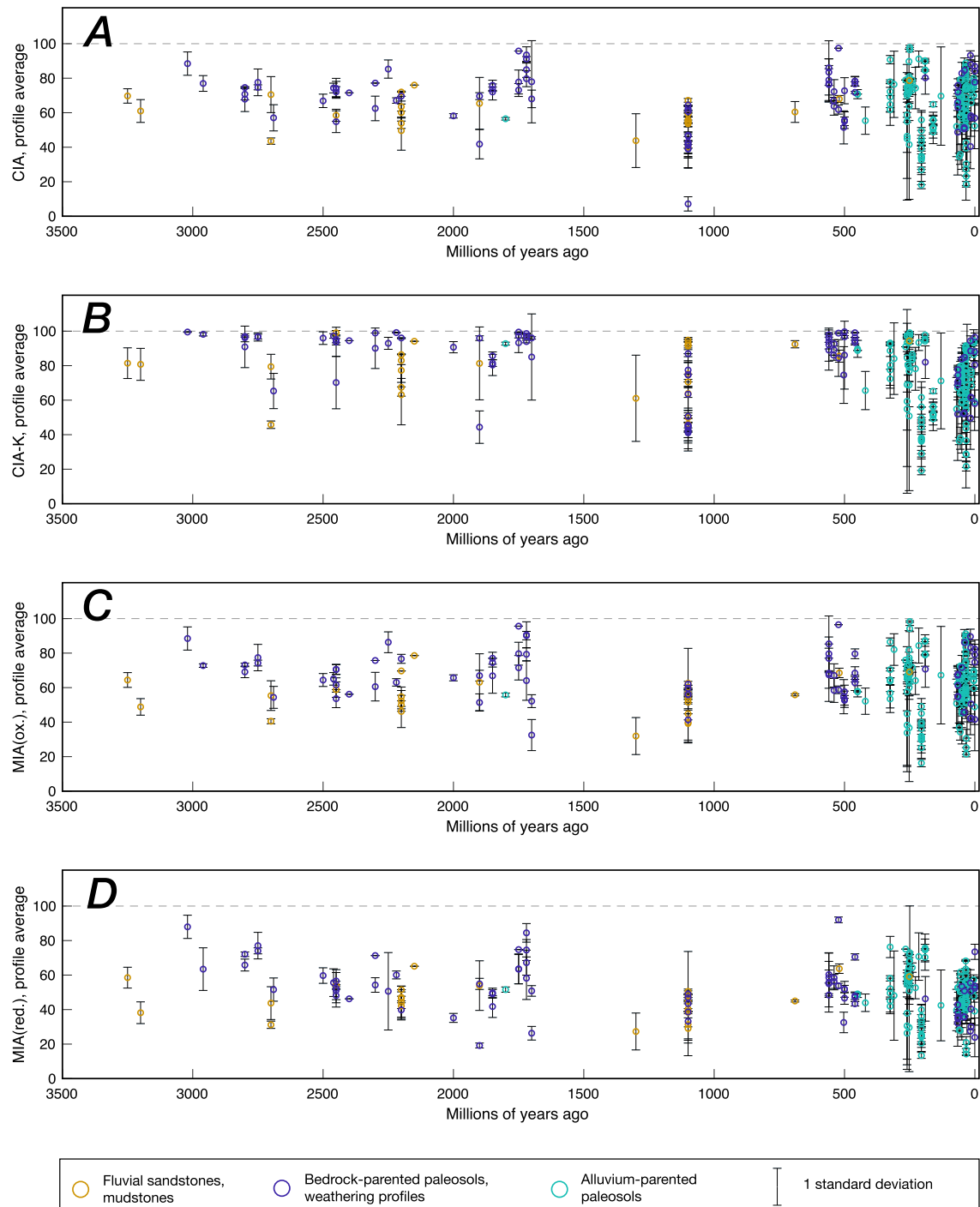


**Fig. 3.** Weathering indices in paleosols (profile averages) through time, where purple dots are bedrock-parented paleosols ( $n = 85$ ), teal dots are alluvium-parented paleosols ( $n = 138$ ), and gold dots are undifferentiated fluvial sandstones and mudstones ( $n = 25$ ). Error bars represent  $1\sigma$  within an individual profile. (A) CIA, (B) CIA-K, (C), MIA<sub>oxic</sub>, and (D) MIA<sub>reducing</sub>. Gray dashed line in all marks CIA = 100, the maximum value. Only error bars extend beyond this threshold.

$$\text{MIA(ox.)} = (\text{Al}_2\text{O}_3 + \text{Fe}_2\text{O}_3) / (\text{Al}_2\text{O}_3 + \text{Fe}_2\text{O}_3 + \text{MgO} + \text{CaO} + \text{Na}_2\text{O} + \text{K}_2\text{O}) * 100 \quad (3)$$

$$\text{MIA(red.)} = \text{Al}_2\text{O}_3 / (\text{Al}_2\text{O}_3 + \text{Fe}_2\text{O}_3 + \text{MgO} + \text{CaO} + \text{Na}_2\text{O} + \text{K}_2\text{O}) * 100 \quad (4)$$

While weathering index values were calculated for all samples, we only used values from the upper portion of a paleosol or weathering profile (i.e., A/B horizon for Phanerozoic paleosols, above

corestones or weakly-weathered parent material for Precambrian weathering profiles) for comparisons to parent material. Individual samples (rather than profile averages) were used for bootstrap resampling or in other analyses where overall variation in paleosol geochemistry was of interest. Because CaO concentration tends to be a primary driver of variability in CIA(-K) and use of the proxy requires CaO screening, we explored CIA both with and without CaO screening (exclusion of samples with CaO > 5%; Dzombak et al., 2021; Michel et al., 2022; Prochnow et al., 2006).

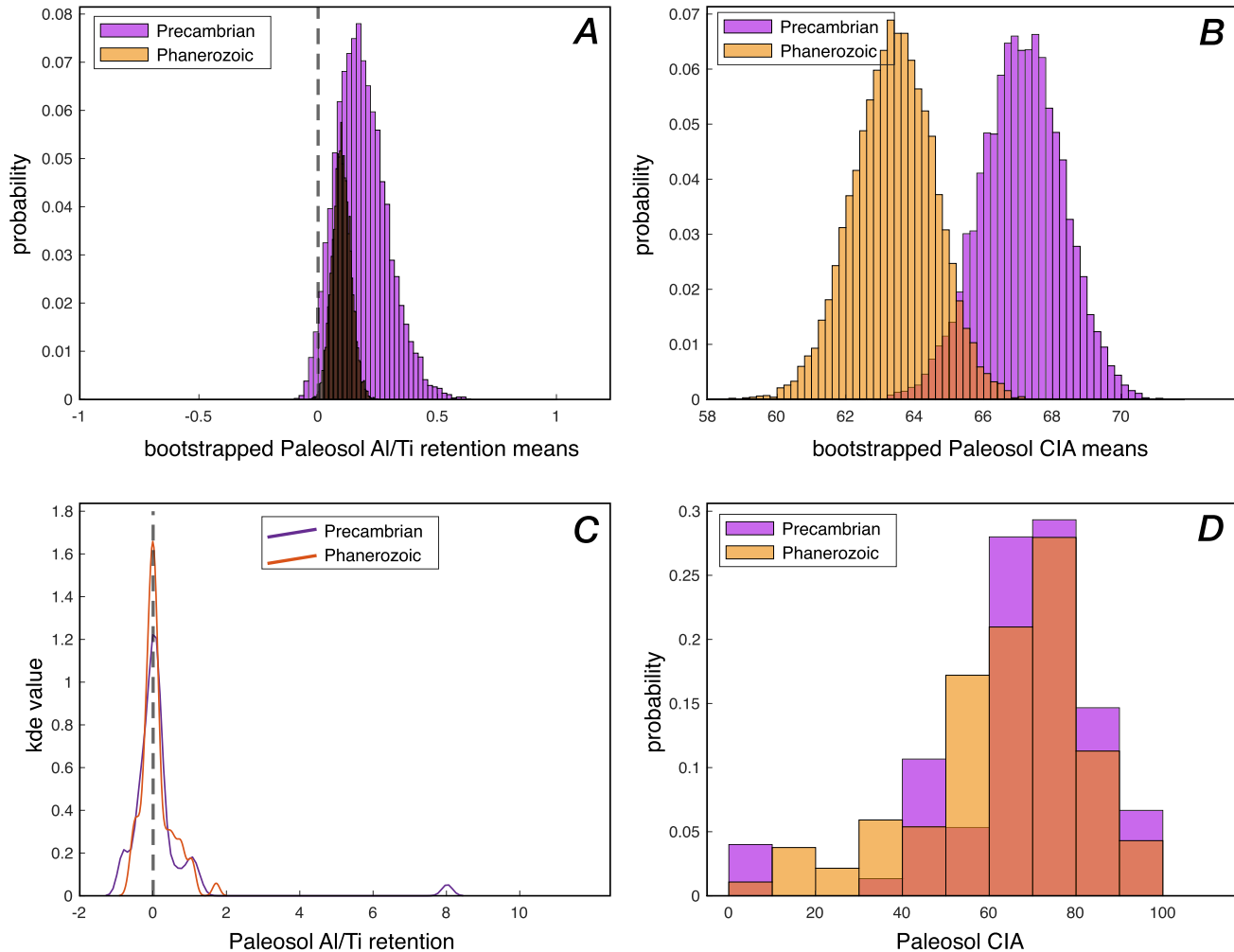


**Fig. 4.** Bootstrap resampled means of (A) Al/Ti retention and (B) CIA values in paleosols (individual samples), binned into Precambrian (purple) and Phanerozoic samples (orange). Note x-axis scale for (B) is 58–72. (C) Kernel density estimates for Al/Ti retention in paleosols (individual samples) in Precambrian (purple) and Phanerozoic (orange) time bins, with both distributions centered on 0 (dashed line; no retention/loss). (D) Histograms of Precambrian (purple) and Phanerozoic (orange) CIA values in paleosols (individual samples), normalized to probability.

For profiles where complete bulk geochemical data were available, we also calculated enrichment/depletion in the ratio of Al/Ti in paleosols relative to their parent material [Eq. (5)], following [Beatty and Planavsky \(2021\)](#). Al is mobilized primarily by organic acids in soils, so examining its relative mobility through time can be a test for weathering due to the presence of an active terrestrial biosphere.

$$\text{Al/Ti retention} = (\text{Al/Ti}_{\text{paleosolavg}}) / (\text{Al/Ti}_{\text{parentavg}}) \quad (5)$$

To contextualize both this ratio and other weathering indices, and to test for possible influences of secular evolution in the composition of continental crust, we also calculated Ti/Al for each individual profile (to test for single profile provenance changes; [Sheldon and Tabor, 2009](#)) and ran time-binned bootstrap resampling for Ti, Al, and Al/Ti through time.

### 2.3. Data distributions and bootstrap analyses

Geochemical data were resampled using a Monte Carlo bootstrapping method to compare between time periods and sample types following [Reinhard et al. \(2017\)](#). Resampling ( $n = 10,000$ , with replacement) showed that while shale means increase slightly, the expansion in range increases, as found in the original

work ([Reinhard et al., 2017](#)). Violin plots of distributions in modern soils and paleosols were generated in Matlab based on [Bechtold \(2016\)](#).

## 3. Results

### 3.1. Weathering through time

Continental weathering intensity has been posited to have undergone state changes (increases) at several points in Earth's history as outlined above. Three key periods commonly proposed to have experienced changes in weathering intensity are around the GOE, as  $p\text{CO}_2$  decreased and  $p\text{O}_2$  increased (ca 2.4–2.2 Ga) ([Lyons et al., 2014](#)), in the Neoproterozoic due to major oscillations in global climate (i.e., Snowball Earth glaciations), and in the Phanerozoic during the evolution of land plants with roots, mycorrhizal fungi, and organic acid weathering ([Neaman et al., 2005](#); [Horodyskyj et al., 2012](#); [Fig. 2b](#)). However, during none of these periods is there a significant increase in weathering indices examined here ([Fig. 2b](#), [Supplemental Fig. 1,2](#)) or by bootstrap resampling of their means ([Fig. 3a,b](#), [Supplemental Fig. 2](#)). Paleosols and weathering profiles do not show a statistically significant shift in average weathering intensity through time

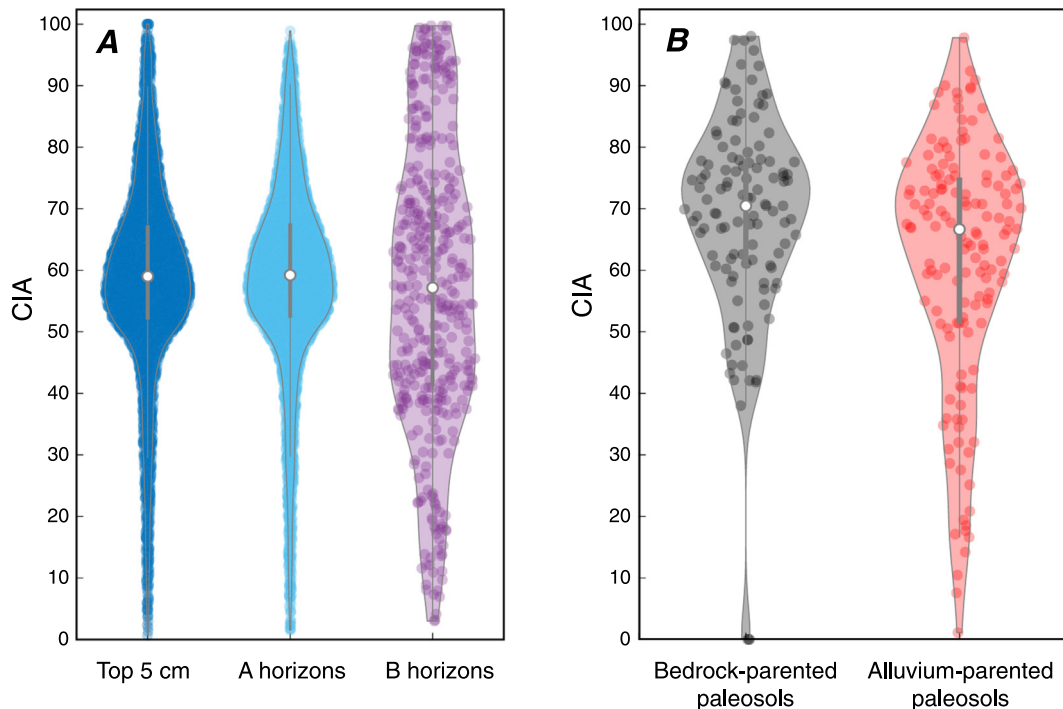


**Fig. 5.** Distributions of CIA values in (A) modern soils and (B) combined Precambrian and Phanerozoic paleosols (profile averages). In all plots, the white dot represents the median value and grey bars are first and third quartiles. The plots' shapes overall suggest normal distributions, with modern B horizons somewhat closer to uniform (Hintze and Nelson, 1998). (Modern soils are compiled in Dzombak and Sheldon, 2020.).

(Fig. 2b; Supplemental Fig. 1). Both raw distributions and bootstrap resampled means' distributions overlap, indicating that the means are within standard error of each other and therefore statistically similar (the Phanerozoic increase in CIA range is geologically meaningful, but not statistically significant). Compared to the distribution of CIA values in modern soils, distribution seen in Phanerozoic paleosols' CIA is similar but with fewer low weathering intensity values preserved during the Precambrian (Fig. 5). Between paleosols and modern soils, paleosols have higher median CIA values by ca. 10 CIA units, and bedrock-parented paleosols in particular have a smaller range, with almost no CIA values <30 (Fig. 5). Tillites have a smaller range of weathering intensities than paleosols and weathering profiles (ca. 40–100; Fig. 6).

In paleosols, Al/Ti is relatively constant and enriched relative to parent material through time (Fig. 7), supporting the results of Beaty and Planavsky (2021) who found similar stability with a smaller set of paleosols. Modern soils have a larger range of Al/Ti retention (higher values) than in paleosols, but all paleosol Al/Ti retention values fall within that range (Fig. 8). Resampled means for Al/Ti in paleosols decrease between the Precambrian and Phanerozoic, while still reflecting retention rather than depletion as the dominant mode (Fig. 8a). The resampled means for  $\text{TiO}_2$  show no meaningful change between the Precambrian and Phanerozoic (Fig. 8a), and resampled means for  $\text{Al}_2\text{O}_3$  decrease in the Phanerozoic from ca. 17.75 to 13.75%  $\text{Al}_2\text{O}_3$  (Fig. 8b,c; Supplemental Fig. 3).

In this compilation, the maximum thickness in Precambrian weathering profiles is higher than Phanerozoic paleosol profiles, which have a larger overall range but lack very thick profiles (Supplemental Fig. 4); however, see discussion on this point below.

### 3.2. Distribution of soil orders through time

For the most part, the literature refrains from describing Precambrian weathering profiles with modern soil taxonomy; most

would likely classify as Entisols based upon a lack of well-defined subsurface horizons, and many (particularly prior to ca. 2.0 Ga ago) are described as laterites/lateritic weathering profiles. In this record (Fig. 2c), the earliest modern soil orders identified are Entisols and Oxisols, both occurring by the Neoproterozoic (Supplemental Table 2). Bandopadhyay et al. (1981) interpreted the 3.02 Ga Keonjhar paleosol as Vertic. Driese (2004) interpreted the 2.2 Ga Hekpoort paleosol as Vertic; Buick et al. 1995 interpreted it as an Oxisol. Gay and Grandstaff (1980) described the 2.3 Ga Pronto paleosol as Spodic. The Neoproterozoic 'Baltic paleosol' profiles (Liivamagi et al., 2015) have been designated as Oxisols. In the Phanerozoic, Vertisols make an appearance at 450 Ma (Beans Gap, TN; Driese and Foreman, 1991). Histosols are sparse in this compilation, with the earliest at 323 Ma (Pennington Fm., KY; Kahmann et al., 2008), but the earliest coals date to the early Devonian (Kidston and Lang, 1921; Krassilov, 1981; see Retallack et al., 1996 for a history of coals). Inceptisols, Alfisols, Ultisols, and Aridisols all occur following ca. 320 Ma in this compilation, but they existed prior to then and are not captured by this compilation (e.g., Morris et al., 2015). Mollisols first appear in this compilation at 33 Ma but are far more extensive in the isotope-only literature for their common carbonate analysis. No Gelisols are present in this record.

## 4. Discussion

### 4.1. What does a stable weathering paleosol record mean?

Our finding of stability in the paleosol weathering record is supported by previous findings of long-term, stable weathering intensity in a smaller paleosol compilation (Beaty and Planavsky, 2021) and in a large but non-specific analysis of sedimentary rocks (Lipp et al., 2021). Lipp et al. (2021) found a stable weathering record in sedimentary rocks from ca. 2.0 Ga ago onward, with shorter-timescale perturbations connected to

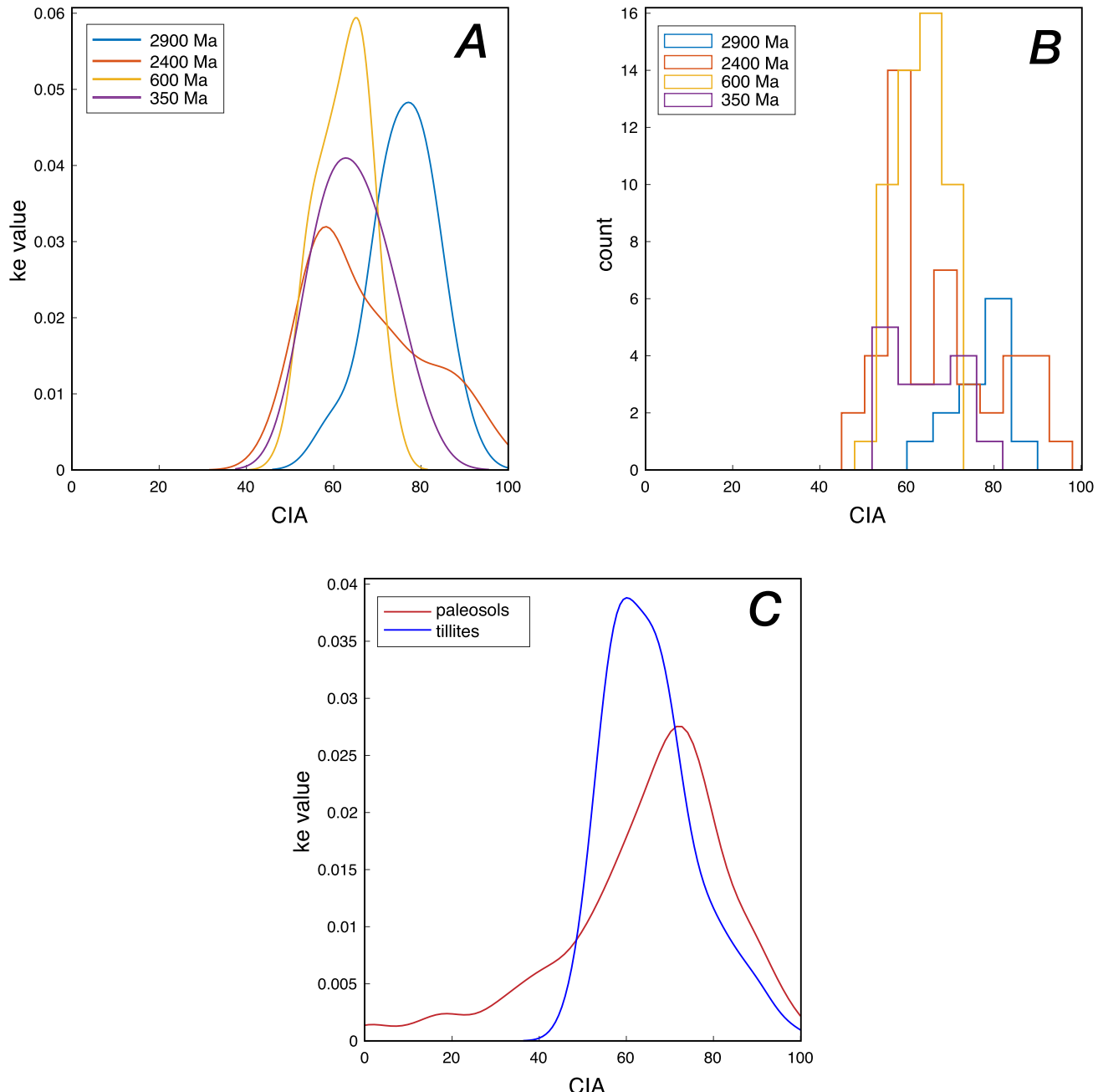


**Fig. 6.** (A) Kernel density estimates for CIA values in glacial tillites from [Gaschnig et al. \(2014\)](#). (B) Histograms of CIA values in glacial tillites from [Gaschnig et al. \(2014\)](#). (C) Kernel density estimates for CIA values in paleosols (red line; this work) and tillites (blue line; [Gaschnig et al. 2014](#)). Tillites have a tighter distribution and generally represent lower weathering intensity than paleosols, but notably lack CIA values  $< 40$  whereas paleosols preserve those.

changes in climate. They posit that transient perturbations in the carbon cycle, with returns to a balanced system, explain the stability of weathering as recorded in shales. The stability in our paleosol record supports the idea of long-term dynamic stability in the carbon cycle with varying strength of silicate weathering–carbon feedbacks (e.g., [Caves et al., 2016](#); see [Berner 2012](#) for a review of the history of these concepts). It has been assumed that the intensity of continental weathering has substantially changed throughout Earth's history as the atmosphere (e.g., high  $p\text{CO}_2$ ), climate (e.g., hothouse versus glacial conditions), tectonics (e.g., supercontinent cycle, orogenesis), and biosphere (e.g., rooted plants, bioturbation) changed. In contrast to expected

variability, the weathering indices analyzed here (CIA, MIA,  $\text{Al}/\text{Ti}$ ) reflect stable weathering intensity in different pedogenic processes through the past 3 Ga, with a Phanerozoic appearance of low-CIA likely driven by the evolution of pedogenesis and appearance of pedogenic carbonate rather than solely by weathering intensity ([Fig. 2b](#)). The terrestrial weathering records compiled here do not reflect discrete, stepped transitions in weathering intensity, but rather an almost modern range of variability in weathering centered about a largely invariant average weathering intensity. This could suggest a trade-off of dominant weathering driver (e.g., transition from climate to biosphere; see [Section 4.3](#)).

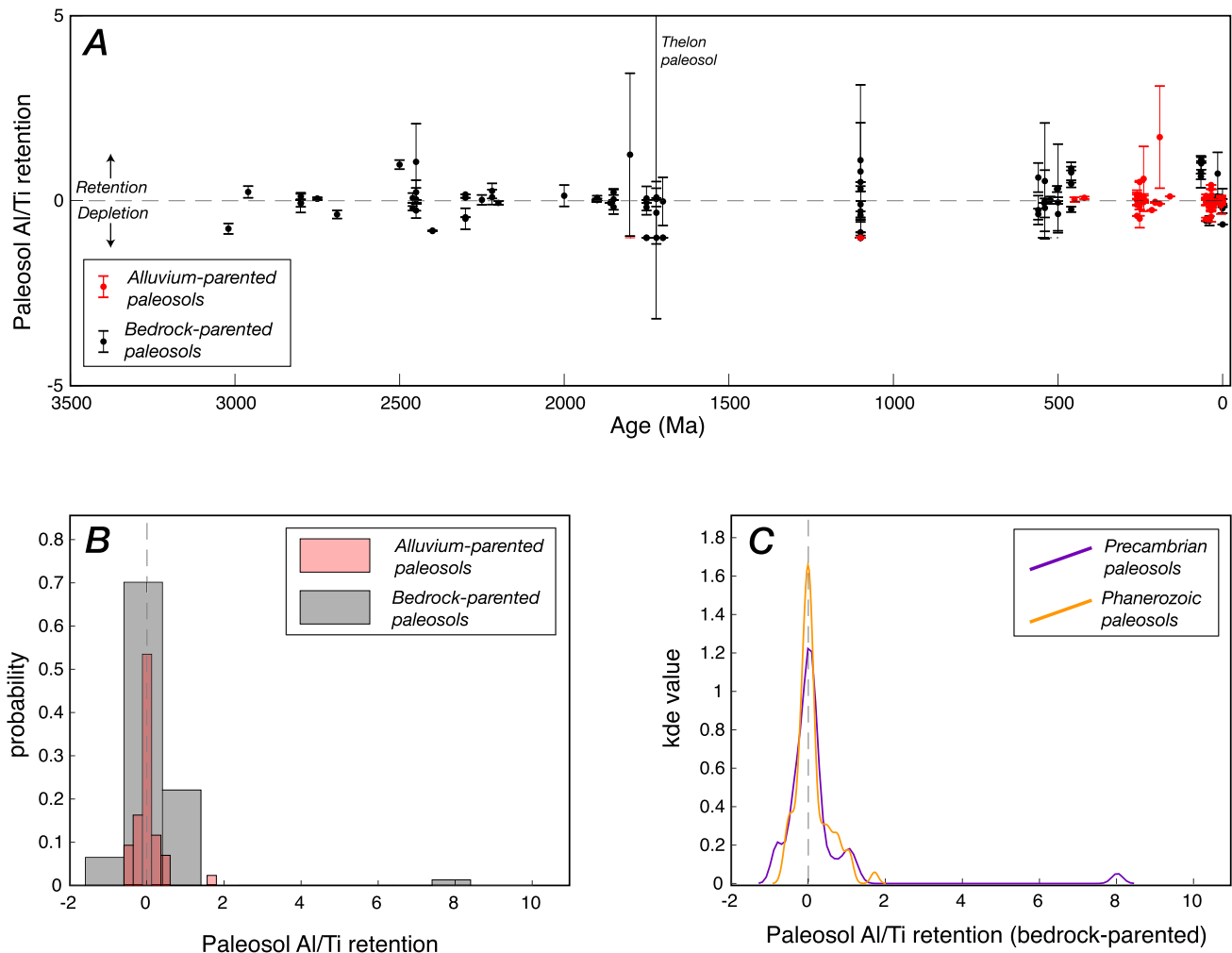


**Fig. 7.** (A) Al/Ti retention/depletion in paleosols (upper profile averages) through time, showing similar results as in [Beatty and Planavsky \(2021\)](#). Dashed line at 0 represents no change between Al/Ti in paleosols vs. parent material. Error bars represent  $1\sigma$  of Al/Ti in an individual profile. One profile (Thelon, bedrock-parented; [Gall, 1994](#)) is not shown at Al/Ti  $\sim 8$ . (B) Probability-normalized histogram of Al/Ti retention in paleosols, binned by parent material. (C) Kernel density estimates for Al/Ti retention in Precambrian (purple line) and Phanerozoic (orange line) paleosols.

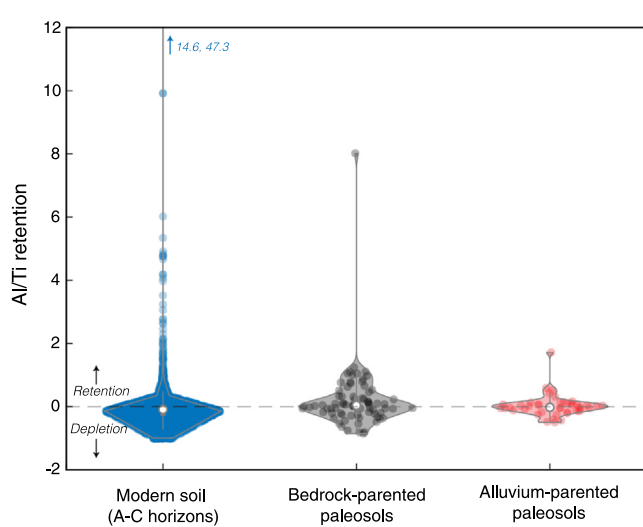


**Fig. 8.** Al/Ti retention in modern soils (leftmost violin plot), bedrock-parented paleosols (middle plot), and alluvium-parented paleosols (rightmost plot). Dashed line at 0 represents no change in Al/Ti between paleosol and parent material. Paleosol points are individual samples.

An additional consideration in interpreting the record of CIA through time is the difference in average CIA value between modern soils and paleosols (around 10 CIA units, [Fig. 5](#)). This lower modern mean could be explained by increased occurrence and preservation of carbonate minerals in very modern soils; it could also be due to a postglacial bias in the dataset of modern soils, with most representing ca. 100 ka at most and many likely reflecting tens of thousands of years. Relatively short periods of soil formation could result in modern soils being less intensely weathered or developed, biasing the CIA record slightly lower. Higher  $p\text{CO}_2$  throughout most of geologic time than in the Quaternary could also contribute to this pattern ([Sheldon et al., 2021](#)). As the Phanerozoic paleosol weathering record is filled in to be more complete, closer examinations of possible correlations between variability in  $p\text{CO}_2$  and terrestrial weathering intensity would be useful in testing the role atmosphere plays in modern-style pedogenesis, as well as how tectonic activity and the creation of accommodation space affect preservation. As that record gets filled in, some of the perturbations seen in the [Lipp et al. \(2021\)](#) sedimentary weathering record could become detectable in paleosols.

We interpret the paleosol weathering records in two primary contexts: the timescale of perturbations in weathering intensity and the shift of dominant control on weathering intensity through

time, including changes in pedogenic mode. We suggest that a baseline level of terrestrial weathering was reached once continents were subaerially exposed and the atmosphere was consistently oxidizing. Once continental weathering was established, perturbations in global weathering intensity occurred but did not lead to discrete, unidirectional state changes as hypothesized. Rather, the weathering record reflects the variability in and evolution of soil-forming factors over time (biosphere, climate, tectonics), with continental area controlling the magnitude of weathering-driven sediment fluxes. Soil formation times and preservation biases obfuscate potential shorter-timescale changes in weathering intensity (e.g., rapid climate change, soils during glacial periods). Additionally, the Phanerozoic increase in the range of CIA values preserved (due to a change in style of pedogenesis and the spread of plants into drier settings where carbonate-bearing Aridisols are formed (e.g., Sheldon and Tabor, 2009), rather than solely reflecting weathering intensity) suggests the value of examining multiple weathering indices.

A key takeaway from the stability of the terrestrial weathering record is the importance of the area of subaerially exposed continent as a primary, baseline control on potential weathering-driven elemental fluxes, as outlined previously by others (e.g., Hao et al., 2017, 2020). If weathering intensity is relatively consistent through time and on geologic timescales, total weatherable area (i.e., subaerially exposed continent) would therefore pose a first-order control on how much sediment would be mobilized via weathering. Lithology of that area (e.g., felsic versus mafic) could be an important factor in global average weathering intensity at a given time (e.g., Lipp et al., 2021; see Section 4.4.5).

#### 4.2. Timescales of weathering intensity events and the geologic baseline

Considering the relevant timescale of interest is important for examining changes in terrestrial weathering intensity. There are numerous, well-constrained, rapid changes in continental weathering intensity throughout the Phanerozoic recorded by paleosols (e.g., Bestland et al., 1997; Sheldon, 2006b; Sheldon et al., 2012; Schaller et al., 2014; Hyland et al., 2017), demonstrating that such events can be captured by paleosols with their relatively short formation times (ca. <100 ka) and over periods of a few million years. In the context of the geologic timescale, however, the weathering signatures of such events effectively get swamped by the long-term signal, which is, for the Phanerozoic, the full range of possible weathering intensity (CIA values of 1–100). Although these rapid events do not appear to affect the long-term trend in terrestrial weathering significantly, they remain important when considered in their relative timescale of interest (typically hundreds of thousands to millions of years) and in the context of other major perturbations at the time (e.g., icehouse/hothouse transition, mass extinction, flood basalts, etc.). As with any index or proxy application, considering apparent changes in the context of uncertainty and background levels of variability is the most robust approach to paleosol geochemistry. The same logic can apply to other perturbations in weathering intensity (tectonic, biotic, etc.) where there is a mismatch between rates of those processes, pedogenesis, and soil preservation.

We interpret the paleosol weathering record presented here to reflect the global 'background' weathering intensity for most of geologic history, setting the baseline for potential sediment fluxes on long timescales. This 'long-term baseline' interpretation supports the findings of Lipp et al. (2021), who used  $\text{CO}_2$  mass-balance and a global compilation of shales (the sediment sink) to estimate weathering intensity over 4 billion years. Their  $\text{CO}_2$  sequestration-based calculations found weathering to be in a steady state on timescales of ca. 0.5 billion years and longer, with

weathering fluxes driven by total amount of erosion, rather than changes in weathering intensity, on long timescales. On shorter timescales (ca. millions of years), weathering and erosion fluxes may have been influenced by more discrete perturbations (e.g.,  $\text{pCO}_2$  fluctuations, climate transitions, tectonics). Such perturbations could have been both spatially and temporally localized. Very short perturbations (<1 Ma) may not be captured by paleosols due to soil formation times, which at their longest typically span the order of 100 ka (Markewich et al., 1990; Sheldon and Tabor, 2009), or by shales, where time-averaging and seafloor erosion could obfuscate the signal that might be better recorded by carbonates.

It is important to note that since at least the beginning of the Phanerozoic, the modern range of weathering intensity is represented in the paleosol CIA record (Fig. 2b). This supports arguments for 'modern' pedogenesis beginning in the Phanerozoic, when vascular, rooting plants evolved and pedogenic carbonate consistently appears in the rock record (e.g., Cerling, 1991; Sheldon and Tabor, 2009; Jolivet and Boulvais, 2021). It is also possible that the Precambrian record suffers from preservation biases leading to low-weathering intensity paleosols (and likely thin or unrecognized as weathering surfaces) being omitted. The MIA record reflects a modern range ca. 1.7 Ga ago, earlier than the CIA record (Fig. 4c, d), and is less influenced by  $\text{CaO}$  concentrations than CIA because it considers more elements. Having this context is necessary for interpreting potential changes in weathering intensity (e.g., up-section variability in CIA) and points to the importance of high-resolution sampling and consideration of error and uncertainty (e.g., Heimsath and Burke, 2013; Hyland and Sheldon, 2016; Amorosi et al., 2021; Dzombak et al., 2021), to avoid over-interpreting a relatively small change in a weathering index. A broader context and preservation biases should always be considered and looking at relative (rather than absolute) changes may be a more appropriate approach to small-scale questions of weathering changes (Bahlburg and Dobrzinski, 2011; Sheldon et al., 2012; Dzombak et al., 2021).

#### 4.3. Changes in dominant weathering mechanisms over time

Stability in the terrestrial weathering record does not mean pedogenesis and continental environments were static through time; rather, we interpret it as supporting a dynamic equilibrium in global tectonic-climate-silicate weathering feedbacks over geologic time. The dominant control or controls on weathering intensity likely varied through time, as the atmosphere evolved, the terrestrial biosphere expanded, and tectonic activity waxed and waned. For example, on the Archean Earth, under high  $\text{pCO}_2$  and with relatively little terrestrial biosphere, terrestrial weathering could have been largely controlled by  $\text{CO}_2$ -dominated weathering (Sheldon, 2006a; Sheldon, 2013). Pedogenesis is generally considered to have changed as these weathering variables evolved through time, shifting first from abiotic  $\text{CO}_2$  acid weathering to both acid and oxidative weathering at the Great Oxygenation Event around 2.4–2.2 Ga (Fig. 1a). There is evidence that by the end of the Archean, organic acid weathering was occurring due to the presence of a terrestrial (microbial) biosphere, contributing to early leaching and weathering profile formation (Rye and Holland, 2000; Driese et al., 2011; Beatty and Planavsky, 2021). An increase in the total diversity of redox-sensitive minerals (i.e., clays, oxides, and oxyhydroxides) has also been used as evidence for changes in oxidative weathering through time (Kennedy et al., 2006; Hazen et al., 2008).

Once weathering mechanisms stabilized as the atmosphere was dominantly oxic and continents were consistently emerged, transient or shorter-term shifts in the driver of weathering intensity would have changed over both space and time. As  $\text{pCO}_2$  dropped

from bars of  $\text{CO}_2$  to thousands of ppm of  $\text{CO}_2$  (Kasting, 1993; Kanzaki and Murakami, 2015; Sheldon et al., 2021) and tectonic activity increased, tectonics may have begun to play a more important role in weathering rate than  $p\text{CO}_2$  by delivering high volumes of readily-weatherable material to the surface (see Section 4.4.6 for LIPs and volcanic arcs). Similarly, as the terrestrial biosphere expanded and global climates alternated between glacial and hot-house periods, those may have increased their contribution to the global weathering intensity signature, trading off as one waxed and the other waned. Climate and relief would also have played different roles in weathering intensity (and therefore soil production) and soil erosion through space and time, contributing variability in paleosol geochemistry, thickness, and preservation (e.g., Dixon et al., 2009; Dixon and von Blanckenburg, 2012; West, 2012; Cao et al., 2019). The overall effect of this continuous interplay of factors could have resulted in the seemingly stable weathering intensity reflected in this compilation.

A final consideration is how these results might be applicable to the study of other planets in the Solar System or eventually, exoplanets. For example, while there is a substantial literature of the geomorphology of Mars and of its changing surface environments (e.g., Smith et al., 1999) and of the surface mineralogy (e.g., Chevrier and Mathé, 2007), until recently, it has only been through analogue experiments (e.g., Baron et al., 2019) that Martian weathering processes have been explored in detail. The ongoing Perseverance mission and the future sample return missions will make direct comparison between early Earth and early Mars weathering possible through databases like the one compiled here.

#### 4.4. Distribution through time and biases in the paleosol record

Several biases related to paleosol soil formation and preservation complicate the interpretation of weathering records on geologic timescales. We note that while this compilation is the largest to date, it is not exhaustive and only includes paleosols and weathering profiles with the relevant bulk geochemical data available. In the Phanerozoic, paleosol studies with isotope data, rather than bulk geochemistry, are more common. These biases are evident in the gaps in the distribution of paleosols (Fig. 2a) as well as trends in paleosol geochemistry, and we discuss each potential source of bias here.

##### 4.4.1. Weathering profile and paleosol thickness through time

Because this record is limited to paleosols and weathering profiles with bulk geochemical data available, we hesitate to draw strong conclusions about changes in soil profile thickness through time (Supplemental Fig. 4). One potential trend is an increase in the range of soil profile thicknesses preserved in the Phanerozoic as compared to the Precambrian, with thinner (often stacked/composite) paleosols more likely to be preserved. This could be due to the Sadler effect (Sadler et al., 1999), the evolution of terrestrial geomorphology, sampling bias, or a combination of those factors. While the record needs to be improved before drawing conclusions about profile thicknesses, we note its importance for understanding the evolution of pedogenesis through time—a critical step for interpreting the paleosol record—and for points of comparison to modern soils and pedogenesis. The thickness of certain Precambrian weathering profiles has been noted with interest, perhaps being reflective of prolonged periods of exposure; however, deep weathering profiles ( $>10$  m) exist in a range of environments today as well (e.g., Nott, 1994; Modenesi-Gauttieri et al., 2011; Hewawasam et al., 2013; Olesen et al., 2013; Regmi et al., 2014; Biondino et al., 2020). Therefore, we should be conservative in interpreting trends in profile thickness before we constrain the true range of both modern soil and paleosol profile thicknesses.

##### 4.4.2. Paleosol bias and climate

Changes in climate (temperature, precipitation, seasonality) can cause perturbations in global weathering and erosion intensity (e.g., Jenny, 1941; Jenny and Amundson, 1994; Bluth and Kump, 1994; Cao et al., 2019). As a primary driver of weathering, climate can facilitate or slow pedogenesis directly (e.g., increased temperature/precipitation) and indirectly (e.g., facilitating terrestrial biosphere). The distribution of climates globally, and the variability of that distribution, fluctuates through time (i.e., the latitudinal temperature gradient in transitional/icehouse conditions vs. stable greenhouse). Based on the weathering records presented here, these changes likely occurred on geologically short timescales (e.g., the Paleocene-Eocene Thermal Maximum, mass extinction events, etc.) or in spatially limited settings (e.g., basin-wide), making such discrete events unlikely to be captured by a coarse or generalized paleosol compilation such as the one presented here. However, basin-scale records with sufficient temporal resolution certainly may reflect rapid or intense changes in weathering intensity (e.g., Sheldon et al., 2012; Hyland et al., 2017; Pogge von Strandmann et al., 2021). Climate would also have affected soil preservation through weathering-erosion relationships (see Section 4.4.4).

Global glaciations and icehouse-greenhouse transitions are the primary exception to the short-term impact of climate on soil formation and preservation, as evidenced by the significant gap in the paleosol record during Neoproterozoic glaciations, although some weathering can still occur during glacial periods (Fig. 2b). While weathering likely slows during global glacial periods, studies of modern glacial environments suggest that chemical weathering at the surface would have continued, even if those terrestrial records were ultimately lost (e.g., Dubnick et al., 2017; Graly et al., 2020; Martin et al., 2020).

##### 4.4.3. Paleosol bias from the biosphere

Prior to the advent of land plants and fungi, the terrestrial biosphere consisted of microbial life, similar to microbial mats and early-stage biological soil crusts present today (e.g., Beraldin-Campesi et al., 2009; Wellman and Strother, 2015). While those communities would have influenced early pedogenesis through organic acid weathering, chemolithotrophy, and landscape stabilization, their potential biosignature may be limited due to erosion and lack of preservation. Compared to the likely impact of rooted plants, particularly roots with symbiotic mycorrhizal fungi, microbial biosignatures could be difficult to detect or establish biogenicity (e.g., Retallack, 2012).

Rooted plants have been hypothesized to have both increased (e.g., Algeo et al., 1995; Algeo and Scheckler, 1998; Lenton and Watson, 2004; Algeo and Twitchett, 2010) or decreased (e.g., D'Antonio et al., 2020) the intensity of terrestrial weathering. They could increase weathering by organic acid weathering enhanced by mycorrhizal fungi (e.g., Lenton and Watson, 2004; Horodyskyj et al., 2012) and physical weathering by roots, or decrease weathering by increasing the volume of soil mantle (therefore shielding bedrock from further weathering; e.g., Burke et al., 2007; Stockmann et al., 2014; Hartmann et al., 2014). Our weathering record and previous work (Beatty and Planavsky 2021; Lipp et al., 2021) show no state change in average weathering intensity during the rise of land plants in the Silurian-Devonian. However, rooting plants could have increased the weathering rate of some elements and minerals (e.g., aluminosilicates) while increasing the retention of elements (e.g., Ca, P; Jobbagy and Jackson, 2001; Horodyskyj et al., 2012), resulting in little net change in average weathering intensity. That balance, and particularly a tendency to accumulate Ca, could also explain the increase in the range of weathering intensities during the Phanerozoic. Some modern soil scientists view soil profiles as existing in a state of plant-stabilized 'dynamic

equilibrium' (e.g., [Lucas, 2001](#)) which lends support to the stability of this record. Additionally, while it is highly likely that rooting land plants altered the overall weathering state and pedogenic style, other competing controls on continental scale weathering intensity could overprint biosphere weathering signatures at times.

The Phanerozoic mean  $\text{Al}_2\text{O}_3$  decrease in the upper portions of paleosols (Supplemental Fig. 3) may reflect increased Al mobility due to plant- and fungi-mediated dissolution ([Hausrath et al., 2009](#); [Beaty and Planavsky, 2021](#)) or a change in the composition of continental crust. The latter is an unlikely explanation; multiple studies have found relatively little change in Archean vs. bulk continental crust, with  $\text{Al}_2\text{O}_3$  estimates for between 14 and 15.2%  $\text{Al}_2\text{O}_3$  throughout geologic history ([Taylor and McLennan, 1985, 1995](#); [Rudnick and Gao, 2003](#); [Lipp et al., 2021](#)). Paleosol Al compositions are approximately centered around the continental crust average (Supplemental Fig. 3), supporting the interpretation of long-term stability at the surface with transient weathering perturbations, and potentially an increase in Al mobility with the advent of rooting by land plants. Geochemical evidence of element mobilization via organic acids is taken as support for fungi-mediated terrestrial weathering due to fungal production of organic acids (e.g., [Lenton and Watson, 2004](#); [Horodyskyj et al., 2012](#)). However, differentiating between fungal acid weathering and plant organic acid weathering (e.g., in the Al/Ti record) without other evidence for the presence of fungi is difficult. Terrestrial fungus species tend to be highly specialized (i.e., forming a symbiosis with a single plant species) due to different plant nutrient needs. To see changes in terrestrial biogeochemistry due to fungi, then, considering plant-specific metal incorporation on a smaller scale might be more appropriate than bulk changes in soil P, regardless of vegetation type. The increase in Al in the Phanerozoic (Supplemental Fig. 3) likely reflects an increase in clay mineral (aluminosilicates) mobility as well. Because clay minerals tend to carry nutrients, an increase in their mobility could have increased marine productivity; however, that increased mobility could also have episodically negatively impacted marine primary productivity by increasing turbidity and reducing light penetration as has been proposed for some Phanerozoic mass extinction events.

#### 4.4.4. Geomorphologic evolution and soil order through time

In the Phanerozoic, paleosol preservation increases, and the number of alluvium-parented paleosols increases as well. Both increases could be due to a combination of preservation bias in which younger rocks are more likely to be preserved than older rocks and fluctuations in sedimentation rate over geologic time ([Sadler et al., 1999](#); [Schumer and Jerolmack, 2009](#); [Meyers and Peters, 2011](#); [Peters and Husson, 2017](#)). If sedimentation and accumulation rates are presumed to fluctuate over time, rather than secularly increase or decrease, the stability of the record remains robust. With more paleosols preserved towards the present and with those paleosols tending to have a wider range of weathering intensities (i.e., retaining the low-CIA values), it is reasonable to expect that if more paleosols were preserved in earlier periods, they would be more likely to capture a wider range of weathering conditions as well. However, preservation biases and the lack of carbonate prior to the Phanerozoic (either from a lack of rooting land plants, higher  $\text{pCO}_2$ , or both) create the CIA record presented here.

The complex relationships between soil production rates, soil thickness, and erosion rates observed in modern soils could also be considered in interpreting paleosols and understanding the evolution of pedogenesis through geologic time. When a soil mantle is present, it tends to decrease the degree of weathering intensity in the bedrock, a relationship that could affect the paleosol weathering record (e.g., [Burke et al., 2007](#); [Goddéris et al., 2008](#); [West, 2012](#); [Stockmann et al., 2014](#); see also Section 10 in [Goudie and](#)

[Viles, 2012](#)). Additionally, high erosion rates beyond a certain threshold tend to correlate with lower weathering intensity on average (see [Dixon and von Blanckenburg, 2012](#)). Because soil thickness, weathering intensity, and erosion can all be impacted by conflated factors such as climate and tectonics that would also vary with the supercontinent cycle (and indeed the complexity and distribution of terrestrial landscapes), these soil thickness-weathering-erosion relationships and controls likely varied through time (as an additional 'changing weathering mechanism' to covary). This point becomes increasingly important because paleosols may be preserved preferentially during one part of the supercontinent cycle ([Dzombak, 2021](#)). The relative relationships may have been different during stable cratonic periods (e.g., [Millot et al., 2002](#)) and varied as alluvium- or regolith-parented soils (rather than bedrock-parented) became more common (e.g., [Phillips, 2010](#); [Norton et al., 2014](#)). Therefore, as our understanding of those factors evolves, preservation biases due to geomorphic evolution should be reconsidered. An in-depth analysis and discussion of these complex interactions is beyond the scope of this work but is an interesting point for future study.

As climate, biosphere, and depositional environments evolved, so too did the range of soils it was possible to form. Although this record is incomplete, we can use it to improve upon previous purely qualitative efforts at constraining the appearance of various soil orders through time ([Retallack, 2001](#)). Some orders tend to be over-represented in the compilation, likely due to a combination of preservation, formation, preservation, and sampling biases (e.g., Vertisols being associated with mountain-building events and of particular interest to parts of the paleosol community). For the record of soil order through time, though, it is essential to consider soil formation and preservation biases. Some soils, such as Gelisols, form in environments that are spatially limited and unlikely to preserve (i.e., thin soils in cold environments). Considering modern depositional environments and soil formation, it is likely that, like the small percentage of marine particles that are eventually preserved on the seafloor, a small subset of soils that ever existed are preserved in the rock record.

Stacked or composite paleosols become more dominant during the Phanerozoic (see Supplemental Table 2; [Kraus, 1999](#)). Beyond a general preservation bias towards the modern, which is present in essentially all geologic records, this could reflect changes in terrestrial geomorphology (i.e., the influence of plants on forming meandering rivers; [Davies and Gibling, 2010](#); [Davies et al., 2021](#); [Ielpi et al., 2022](#)) and a potential overall increase in the global volume of sediments beginning in the Neoproterozoic ([Husson and Peters, 2017](#)). The rise of deeper rooting by vascular plants during the early Phanerozoic could well have played a role in increasing preservation, especially of thinner profiles that could otherwise be readily eroded, serving as a landscape-stabilizing mechanism.

#### 4.4.5. Weathering in LIPs and volcanic arcs

The emplacements of LIPs occur steadily throughout the geologic record (Fig. 1c; [Ernst et al., 2021](#)), and while volcanic arc activity waxes and wanes with the Wilson cycle ([Macdonald et al., 2019](#)), it contributes a relatively consistent and long wavelength change through time. Because of their relatively consistent presence, and along with the steadiness of the paleosol weathering record (as well as the shale record; [Lipp et al., 2021](#)), we consider these processes to contribute to the baseline of weathering intensity through time, creating relatively transient perturbations in weathering intensity. Timescales of perturbation vary from extreme but rapid events (e.g., mass extinctions associated with LIP emplacement, disturbances lasting hundreds of thousands of years; [Sheldon, 2006b,c](#); [Schaller et al., 2011](#); [Gastaldo et al., 2014](#); [Sayyed, 2014](#); [Schaller et al., 2014](#); [van de Schootbrugge et al., 2020](#); [Longman et al., 2021](#)) to longer changes in the silicate

weathering distribution, on millions of years, as supercontinents assemble and break apart. The precise relationship between LIPs and global weathering (along with climate and the biosphere) is equivocal. LIP emplacement and volcanic arc activity have been posited as primary controls on weathering and erosion (e.g., Macdonald et al., 2019; Sternai et al., 2019; Gernon et al., 2021). Although volcanism associated with LIP emplacement adds atmospheric CO<sub>2</sub>, high weathering rates of the large bodies of fresh basalt may be enough to offset added CO<sub>2</sub> (e.g., Dessert et al., 2003; Dupré et al., 2003; Goddériss et al., 2003). Links between magmatism, topography, and associated climate-topography-erosion forcing could also play a role in weathering rates and volcanic rock bodies as net C sinks (e.g., Lee et al., 2015; Sternai et al., 2019). Thus, it is still an open question of whether LIPs represent a net carbon sink or carbon source; filling out the paleosol record through time and using it to ascertain changes in terrestrial geochemistry may help answer this.

While some key LIP events such as the Deccan Traps (e.g., Dzombak et al., 2020), Central Atlantic Magmatic Province (e.g., Schaller et al., 2011), and Columbia River Flood Basalt Province (e.g., Sheldon, 2006c) preserve intra-basaltic paleosols that can be used to examine relationships between weathering intensity and climate directly (see Sayyed, 2014), adding additional paleosols during other Phanerozoic LIPs could help settle the debate about whether the LIPs enhanced weathering through direct greenhouse gas emissions or by increasing the size of the C sink available for silicate weathering.

#### 4.4.6. Sampling biases in paleosol research

Sampling biases—both in space and time—obfuscate true trends in the paleosol record, as with any field-based sampling. As is evident during the GOE in this record, certain time periods of interest may be over-sampled relative to the number of profiles that exist during that timeframe. Certain soil orders of interest may also be overrepresented; for instance, Vertisols account for nearly a quarter of Phanerozoic profiles in this record, despite forming in a limited range of environments (Vertisols cover only about 2.4% of ice-free land area today; USDA-NRCS, 2005). In the Precambrian, weathering profiles with low weathering intensities may be under-sampled due to low profile thicknesses or simply due to our failure to recognize them as weathering profiles (e.g., they were logged as clastic rocks). This could contribute to the narrower range of weathering intensities in Precambrian profiles. Paleosols yielding pedogenic carbonate (i.e., arid and semi-arid regions) may also be over-sampled for carbon and oxygen isotope analysis (Sheldon and Tabor, 2009; Jolivet and Boulvais, 2021), whereas tropical areas where pedogenic carbonate is unlikely to form or be preserved may be under-sampled. Globally, access to field sites and a history of high-resolution geologic mapping varies widely, typically biasing our knowledge of paleosols to areas with good access and active geologic research. Not all types of data are available for every paleosol or weathering profile, limiting the conclusions that can be drawn from different subsets of a compilation. For example, many paleosol studies focusing on carbonate isotope geochemistry report only those values rather than also reporting bulk oxides, so the record here may under-represent carbonate-bearing paleosols, which would also lead to under-sampling of low CIA values. Considering sampling biases is useful when comparing different types of records (i.e., are they biased in similar ways?) and can make interpretations of geochemical records more robust.

#### 4.5. Implications for reconstructing past climates and biogeochemical cycling

Biogeochemical models inherently include assumptions about the timing, rates, and magnitude of continental weathering and

resultant sediment fluxes to oceans; however, until now, no quantitative record has existed to inform model parameters. Despite the gaps in the paleosol record, this compilation provides a baseline for weathering, suggesting that an essentially modern range of weathering intensities could have occurred at most points during Earth's history. Perhaps because the record reflects this background variability, some transient events that are known to have been captured by paleosols (e.g., the EECO, PETM; Sheldon et al., 2012; Gallagher and Sheldon, 2013; Hyland et al., 2017; Ramos et al., 2022) are not reflected. Therefore, the weathering intensity record could be used as a baseline distribution, with known perturbations essentially shifting the distribution of weathering values higher only for a short time. Models should not necessarily rely on secular or discrete increases in terrestrial weathering as a driver for long-term, biogeochemical state changes. Biogeochemical models should also take the Phanerozoic increase in paleosol CaO into account when modeling Phanerozoic carbon cycling and other connected biogeochemical systems.

An important implication for the practical application of paleosol geochemistry in reconstructing past climates and biogeochemical changes is the need to quantify background variability on the temporal and spatial scales of interest. If, at any given time from 3 Ga ago onwards, a paleosol CIA value could be 0–100, individual profiles are of little use unless they are placed in environmental and tectonic context. Including multiple profiles in space and time, as well as comparing paleosol geochemistry to other proxies (e.g., Tabor et al., 2008; Gulbranson et al., 2015; Hyland and Sheldon, 2016; Hyland et al., 2017; Dzombak et al. 2021; Gulbranson et al., 2022) constrains local to regional geochemical variability and allows more robust interpretation of paleosol geochemical trends. Additionally, considering relative rather than absolute changes may be appropriate if other external factors can only be poorly constrained (e.g., Hyland et al., 2017; Dzombak et al., 2021).

#### 4.6. Next steps

The compilation presented here highlights the need for a collaborative and comprehensive paleosol database that will allow some outstanding “big questions” in the field to be addressed and identifies high-value sampling targets as such a database is built (e.g., Neoproterozoic weathering profiles). The Phanerozoic record in particular should be filled in to robustly test hypotheses related to the rise of land plants and the distribution of soil orders through (relatively recent) geologic time, which would shed light on the distribution of terrestrial ecosystems and depositional environments through time as well. Filling in the Phanerozoic paleosol record could also help elucidate relationships between tectonics, weathering and erosion, and climate, particularly at the basin scale. Additionally, constraining modern soils globally in a similar approach—profile thicknesses, weathering intensity, geochemical composition, etc.—is necessary to provide a baseline or point of reference for interpreting potential trends or changes in the paleosol record. Finally, exploring individual elements in detail—particularly for the Phanerozoic record—could provide unique insights into specific biogeochemical cycles.

#### 5. Conclusions

In contrast with common assumptions about how terrestrial weathering intensity has changed through geologic time, our new compilation shows a stable average in terrestrial weathering intensity in a suite of weathering indices (CIA-K), MIA, and Al/Ti), providing support for two recent long-term weathering records that were stable on long timescales. There were no discrete, step

changes in continental weathering intensity, but rather a range of variability centered about a stable average value. While the weathering indices' averages are similar over the past three billion years, one—CIA—exhibits an increase in range in the Phanerozoic due to the increased presence of low-CIA paleosols. This could suggest a fundamental change in pedogenesis during the Phanerozoic (i.e., the formation of pedogenic carbonate), a preservation and/or sampling bias in lightly weathered Precambrian paleosols, or a combination of the two. We interpret the ~10-unit difference in mean CIA between modern soils and paleosols as a preservation bias imposed by North American glaciation in the late Quaternary.

Overall, these stable records reflect the long-term baseline of terrestrial weathering intensity, which can be perturbed on geologically short timescales (e.g., rapid climate transitions, tectonic events) before returning to its dynamic, steady state. Over geologic time, factors such as supercontinent assembly and breakup, LIP emplacement and volcanic arc activity, climate, and the biosphere likely trade off in dominating the signal of weathering intensity, resulting in a stable average with a large range in variability through time. In this context, subaerially exposed, weatherable land area is a fundamental control on the volume of sediment mobilized through weathering through time, and lithology (mafic, felsic) could contribute to the rate of weathering at a given time for a given area. Biogeochemical models could incorporate the average and range of weathering intensity, and associated uncertainty, when estimating erosional and nutrient fluxes to marine ecosystems through time.

## Declaration of Competing Interest

The authors declare that they have no known competing financial interests or personal relationships that could have appeared to influence the work reported in this paper.

## Acknowledgments

Funding during this work was partially provided by NSF #1812949 to N.D.S and others. Thanks to Jordan Tyo, Katie Seguin, Bianca Gallina, and Sonya Vogel for help in assembling this dataset. Thanks to Erik Gulbranson and an anonymous reviewer for their helpful comments in improving this manuscript.

## Appendix A. Supplementary material

Supplementary data to this article can be found online at <https://doi.org/10.1016/j.gr.2022.05.009>.

## References

Algeo, T.J., Berner, R.A., Maynard, J.B., Scheckler, S.E., 1995. Late Devonian Oceanic Anoxic Events and Biotic Crises: 'Rooted' in the Evolution of Vascular Land Plants? *GSA Today* 5, 145, 64–66.

Algeo, T.J., Scheckler, S.E., 1998. Terrestrial-marine teleconnections in the Devonian: links between the evolution of land plants, weathering processes, and marine anoxic events. *Philos. Trans. R. Soc. London B* 353, 113–130.

Algeo, T.J., Twitchett, R.J., 2010. Anomalous Early Triassic sediment fluxes due to elevated weathering rates and their biological consequences. *Geology* 38, 1023–1026.

Amorosi, A., Bruno, L., Campo, B., Di Martino, A., Sammartino, I., 2021. Patterns of geochemical variability across weakly developed paleosol profiles and their role as regional stratigraphic markers (Upper Pleistocene, Po Plain). *Palaeogeogr. Palaeoclimatol. Palaeoecol.* 574, 110413. <https://doi.org/10.1016/j.palaeo.2021.110413>.

Anbar, A.D., Knoll, A.H., 2002. Proterozoic Ocean Chemistry and Evolution: A Bioinorganic Bridge? *Science* 297, 1137–1142.

Anbar, A.D., Duan, Y., Lyons, T.W., Arnold, G.L., Kendall, B., Creaser, R.A., Kaufman, A.J., Gordon, G.W., Scott, S., Garvin, J., Buick, R., 2007. A whiff of oxygen before the great oxidation event? *Science* 317, 1903–1906.

Babechuk, M.G., Widdowson, M., Kamber, B.S., 2014. Quantifying chemical weathering intensity and trace element release from two contrasting basalt profiles, Deccan Traps, India. *Chem. Geol.* 363, 56–75.

Bahlburg, H., Dobrinski, N., 2011. A review of the Chemical Index of Alteration (CIA) and its application to the study of Neoproterozoic glacial deposits and climate transitions. In: Arnaud, E., Halverson, G.P., Shields-Zhou, G. (Eds.), *The Geological Record of Neoproterozoic Glaciations*, Geol. Soc. Mem., vol. 36, London, pp. 81–92.

Bandopadhyay, P.C., Eriksson, P.G., Roberts, R.J., 1981. A vertic paleosol at the Archean-Proterozoic contact from the Singhbhum-Orissa craton, eastern India. *Precambrian Res.* 17, 277–290.

Baron, F., Gaudin, A., Lorand, J.-P., Mangold, N., 2019. New constraints on early Mars weathering conditions from an experimental approach on crust simulants. *J. Geophys. Res. Plan.* 124, 1783–1801.

Bayon, G., Freslon, N., Germain, Y., Bindeman, I.N., Trinquier, A., Barrat, J.A., 2021. A global survey of radiogenic strontium isotopes in river sediments. *Chem. Geol.* 559, 119958.

Beatty, B.J., Planavsky, N.J., 2021. A 3 b.y. record of a biotic influence on terrestrial weathering. *Geology* 49, 407–411.

Bechtold, B., 2016. Violin plots for Matlab, Githun Project <https://github.com/bastibe/Violinplot-Matlab> <https://doi.org/10.5281/zenodo.4559847>.

Beraldi-Campesi, H., Hartnett, H.E., Anbar, A.D., Gordon, G.W., Garcia-Pichel, F., 2009. Effect of biological soil crusts on soil elemental concentrations: Implications for biogeochemistry and as traceable biosignatures of ancient life on land. *Geobiology* 7, 348–359.

Berner, R.A., 1998. The carbon cycle and CO<sub>2</sub> over Phanerozoic time: The role of land plants. *Phil. Trans. R. Soc. B Biol. Sci.* 353, 75–82.

Berner, R.A., 2004. *The Phanerozoic Carbon Cycle: CO<sub>2</sub> and O<sub>2</sub>*. Oxford University Press, Oxford, UK.

Berner, R.A., 2006. GEOCARBSULF: A combined model for Phanerozoic atmospheric O<sub>2</sub> and CO<sub>2</sub>. *Geochim. Cosmochim. Acta* 70, 5653–5664.

Berner, R.A., 2012. Jacques-Joseph Ébelmen, the founder of Earth system science. *Compt. Rendus Geosci.* 344, 544–548.

Bestland, E.A., Retallack, G.J., Swisher, C.C., 1997. Stepwise climate change recorded in Eocene-Oligocene paleosol sequences from Central Oregon. *J. Geol.* 105, 153–172.

Biondino, D., Borrelli, L., Critelli, S., Muto, F., Apolloaro, C., Coniglio, S., Tripodi, V., Perri, F., 2020. A multidisciplinary approach to investigate weathering processes affecting gneissic rocks (Calabria, southern Italy). *Catena* 187, 104372.

Blum, J.D., Gazis, C.A., Jacobson, A.D., Chamberlain, C.P., 1998. Carbonate versus silicate weathering in the Raikhot watershed within the High Himalayan Crystalline Series. *Geology* 26, 411–414.

Bluth, G.J.S., Kump, L.R., 1994. Lithologic and climatologic controls of river chemistry. *Geochim. Cosmochim. Acta* 58, 2341–2359.

Brass, G.W., 1975. The effect of weathering on the distribution of strontium isotopes in weathering profiles. *Geochim. Cosmochim. Acta* 39, 1647–1653.

Brocks, J.J., Jarrett, A.J.M., Sirantoini, E., Hallman, C., Hoshino, Y., Liyanage, T., 2017. The rise of algae in Cryogenian oceans and the emergence of animals. *Nature* 548, 578–581.

Buick, R., Thronett, J.R., McHaughton, N.J., Smith, J.B., Barley, M.E., Savage, M., 1995. Record of emergent continental crust ~3.5 billion years ago in the Pilbara craton of Australia. *Lett. Nat.* 375, 574–577.

Burke, B.C., Heimsath, A.M., White, A.F., 2007. Coupling chemical weathering with soil production across soil-mantled landscapes. *Earth Surf. Process. Landforms* 32, 853–873.

Campbell, I.H., Squire, R.J., 2010. The mountains that triggered the Late Neoproterozoic increase in oxygen: The second Great Oxidation Event. *Geochim. Cosmochim. Acta* 74, 4187–4206.

Cao, Y., Song, H., Algeo, T.J., Chu, D., Du, Y., Tian, L., Wang, Y., Tong, J., 2019. Intensified chemical weathering during the Permian-Triassic transition recorded in terrestrial and marine successions. *Palaeogeogr. Palaeoclimatol. Palaeoecol.* 519, 166–177.

Carver, J.H., Vardavas, I.M., 1994. Precambrian glaciations and the evolution of the atmosphere. *Ann. Geophys.* 12, 674–682.

Caves, J.K., Jost, A.B., Lau, K.V., Maher, K., 2016. Cenozoic carbon cycle imbalances and a variable weathering feedback. *Earth Plan. Sci. Lett.* 450, 152–163.

Cerling, T.E., 1991. Carbon dioxide in the atmosphere: Evidence from Cenozoic and Mesozoic paleosols. *Am. J. Sci.* 291, 377–400.

Cermeno, P., Falkowski, P.G., Romero, O.E., Schaller, M.F., Vallina, S.M., 2015. Continental erosion and the Cenozoic rise of marine diatoms. *Proc. Natl. Acad. Sci. U.S.A.* 112, 4239–4244.

Chowdhury, P., Mulder, J.A., Cawood, P.A., Mukherjee, S., 2021. Magmatic thickening of crust in non-plate tectonic settings initiated the subaerial rise of Earth's first continents 3.3 to 3.2 billion years ago. *Proc. Natl. Acad. Sci. U. S. A.* 118, e2105746118.

Chevrier, V., Mathé, P.E., 2007. Mineralogy and evolution of the surface of Mars: A review. *Plan. Space Sci.* 55, 289–314.

Cohen, A.S., Coe, A.L., 2002. New geochemical evidence for the onset of volcanism in the Central Atlantic magmatic province and environmental change at the Triassic-Jurassic boundary. *Geology* 30, 267–270.

Colwyn, D.A., Sheldon, N.D., Maynard, J.B., Gaines, R., Hofmann, A., Wang, X., Gueguen, B., Asael, D., Reinhard, C.T., Planavsky, N.J., 2019. A paleosol record of the evolution of Cr redox cycling and evidence for an increase in atmospheric oxygen during the Neoproterozoic. *Geobiology* 17, 579–593.

Cox, G.M., Halverson, G.P., Stevenson, R.K., Vokaty, M., Poirier, A., Kunzmann, M., Li, Z.X., Denyszyn, S.W., Strauss, J.V., Macdonald, F.A., 2016. Continental flood basalt weathering as a trigger for Neoproterozoic Snowball Earth. *Earth Plan. Sci. Lett.* 446, 89–99.

D'Antonio, M.P., Ibarra, D.E., Boyce, C.K., 2020. Land plant evolution decreased, rather than increased, weathering rates. *Geology* 48, 29–33.

Davies, N.S., Gibling, M.R., 2010. Cambrian to Devonian evolution of alluvial systems: The sedimentological impact of the earliest land plants. *Earth-Sci. Rev.* 98, 171–200.

Davies, N.S., Berry, C.M., Marshall, J.E.A., Wellman, C.H., Lindemann, F.J., 2021. The Devonian landscape factory: plant-sediment interactions in the Old Red Sandstone of Svalbard and the rise of vegetation as a biogeomorphic agent. *J. Geol. Soc. 178*. <https://doi.org/10.1144/jgs2020-225>.

Dessert, C., Dupré, B., Gaillardet, J., François, L.M., Allègre, C.J., 2003. Basalt weathering laws and the impact of basalt weathering on the global carbon cycle. *Chem. Geol.* 202, 257–273.

Dixon, J.L., Heimsath, A.M., Kaste, J., Amundson, R., 2009. Climate-driven processes of hillslope weathering. *Geology* 37, 975–978.

Dixon, J.L., von Blanckenburg, F., 2012. Soils as pacemakers and limiters of global silicate weathering. *Compt. Rendus-Geosci.* 344, 597–609.

Domeier, M., Magni, V., Hounslow, M.W., Torsvik, T.H., 2018. Episodic zircon age spectra mimic fluctuations in subduction. *Sci. Rep.* 8, 17471.

Donnadieu, Y., Godderis, Y., Ramstein, G., Nedelec, A., Meert, J., 2004. A 'snowball Earth' climate triggered by continental break-up through changes in runoff. *Nature* 541, 303–306.

Driese, S.G., Foreman, J.L., 1991. Traces and related chemical changes in a Late Ordovician paleosol, *Glossifungites* ichnofacies, southern Appalachians, USA. *Ichnos* 1, 207–219.

Driese, S.G., 2004. Pedogenic translocation of Fe in modern and ancient Vertisols and implications for interpretations of the Hekpoort paleosol (2.25 Ga). *J. Geol.* 112, 543–560.

Driese, S.G., Jirsa, M.A., Ren, M., Brantley, S.L., Sheldon, N.D., Parker, D., Schmitz, M., 2011. Neoproterozoic paleoweathering of tonalite and metabasalt: Implications for reconstructions of 2.69 Ga early terrestrial ecosystems and paleoatmospheric chemistry. *Precam. Res.* 189, 1–17.

Dubnick, A., Wadham, J., Tranter, M., Sharp, M., Orwin, J., Barker, J., Bagshaw, E., Fitzsimons, S., 2017. Trick or treat: The dynamics of nutrient export from polar glaciars. *Hydro. Process.* 31, 1776–1789.

Dupré, B., Dessert, C., Oliva, P., Godderis, Y., Viers, J., François, L., Millot, R., Gaillardet, J., 2003. Rivers, chemical weathering and Earth's climate. *Compt. Rendus-Geosci.* 335, 1141–1160.

Dzombak, R.M., 2021. Geochemical Variability in Fossil Soils and Implications for Past Biogeochemical Cycling, Climates, and Atmospheres. Doctoral dissertation, University of Michigan. <https://doi.org/10.7302/3066>.

Dzombak, R.M., Sheldon, N.D., Mohabey, D.M., Samant, B., 2020. Stable climate in India during Deccan volcanism suggests limited influence on K-Pg extinction. *Gondwana Res.* 85, 19–31.

Dzombak, R.M., Sheldon, N.D., 2020. Weathering intensity and presence of vegetation are key controls on soil phosphorus concentrations: Implications for past and future terrestrial ecosystems. *Soil Sys.* 4, 73.

Dzombak, R.M., Midttun, N.C., Stein, R.A., Sheldon, N.D., 2021. Incorporating lateral variability and extent of paleosols into proxy uncertainty. *Palaeogeogr. Palaeoclim. Palaeoecol.* 582, 110641.

Ernst, R., Bond, D.P.G., Zhang, S.H., Buchan, K.L., Grasby, S.E., Youbi, N., El Bilali, H., Bekker, A., Doucet, L.S., 2021. Part I. The temporal record of large igneous provinces (LIPs). In: Ernst, R.E., Dickson, A.J., Bekker, A. (Eds.), Large Igneous Provinces: A Driver of Global Environmental and Biotic Changes. American Geophysical Union and John Wiley, Sons, Inc., D.C.

Fabre, S., Berger, G., Nédélec, A., 2011. Modeling of continental weathering under high-CO<sub>2</sub> atmospheres during Precambrian times. *Geochem., Geophys., Geos.* 12, 1–23.

Farrell, U.C., Samawi, R., Anjanappa, S., Klykov, R., Adeboye, O.O., Agic, H., Ahm, A.C., Boag, T.H., Bowyer, F., Brocks, J.J., Bruno, T.N., Canfield, D.E., Chen, X., Cheng, M., Clarkson, M.O., Cole, D.B., Cordie, D.R., Crockford, P.W., Cui, H., Dahl, T.W., Mouro, L.D., Dewing, K., Dornbos, S.Q., Drabon, N., Dumoulin, J.A., Emmings, J.F., Endriga, C.R., Fraser, T.A., Gaines, R.R., Gaschnig, R.M., Gibson, T.M., Gilleadeau, G.J., Gill, B.C., Goldberg, K., Guilaub, R., Halverson, G.P., Hammarlund, E.U., Hantsoo, K.G., Henderson, M.A., Hodgeskiss, M.S.W., Horner, T.J., Husson, J.M., Johnson, B., Kabanov, P., Keller, C.B., Kimmig, J., Kipp, M.A., Knoll, A.H., Kreitsmann, T., Kunzmann, M., Kurzweil, F., LeRoy, M.A., Li, C., Lipp, A.G., Loydell, D.K., Lu, X., Macdonald, F.A., Magnall, J.M., Månd, K., Mehra, A., Melchin, M.J., Miller, A.J., Mills, N.T., Mwinde, C.N., O'Connell, B., Och, L.M., Ossa, F., Pagès, A., Paiste, K., Partin, C.A., Peters, S.E., Petrov, P., Playter, T.L., Plaza-Torres, S., Porter, S.M., Poulton, S.W., Pruss, S.B., Richoz, S., Ritzer, S.R., Rooney, A.D., Sahoo, S.K., Schoepfer, S.D., Sclafani, J.A., Shen, Y., Shorttle, O., Slotnick, S.P., Smith, E.F., Spinks, S., Stockey, R.G., Strauss, J.V., Stüeken, E.E., Tecklenburg, S., Thomson, D., Tosca, N.J., Uhlein, G.J., Vizcaino, M.N., Wang, H., White, T., Wilby, P.R., Woltz, C.R., Wood, R.A., Xiang, L., Yurchenko, I.A., Zhang, T., Planavsky, N.J., Lau, K.V., Johnston, D.T., Sperling, E.A., 2021. The sedimentary geochemistry and paleoenvironments project. *Geobiol.* 19, 545–556.

Fedo, C.M., Nesbitt, H.W., Young, G.M., 1995. Unraveling the effects of potassium metasomatism in sedimentary rocks and paleosols, with implications for paleoweathering conditions and provenance. *Geology* 23, 921–924.

Fedo, C.M., Eriksson, K.A., Krogstad, E.J., 1996. Geochemistry of shales from the Archean (~3.0 Ga) Buhu Greenstone Belt, Zimbabwe: Implications for provenance and source-area weathering. *Geochim. Cosmochim. Acta* 60, 1751–1763.

Francois, L.M., Walker, J.C.G., 1992. Modelling the Phanerozoic carbon cycle and climate: constraints from the <sup>87</sup>Sr/<sup>86</sup>Sr isotopic ratio of seawater. *Am. J. Sci.* 292, 81–135.

Gall, Q., 1994. The Proterozoic Thelon paleosol, Northwest Territories, Canada. *Precam. Res.* 68, 15–137.

Gallagher, T.M., Sheldon, N.D., 2013. A new paleothermometer for forest paleosols and its implications for Cenozoic climate. *Geology* 41, 647–650.

Gaschnig, R.M., Rudnick, R.L., McDonough, W.F., Kaufman, A.J., 2014. Onset of oxidative weathering of continents recorded in the geochemistry of ancient glacial diamictites. *Earth Plan. Sci. Lett.* 408, 87–99.

Gastaldo, R.A., Knight, C.L., Neveling, J., Tabor, N.J., 2014. Latest Permian paleosols from Wapadspberg Pass, South Africa: Implications for Changhsingian climate. *Geol. Soc. Am. Bull.* 126, 665–679.

Gay, A.L., Grandstaff, D.E., 1980. Chemistry and mineralogy of Precambrian paleosols at Elliot Lake, Ontario, Canada. *Precam. Res.* 12, 349–373.

Gernon, T.M., Hincks, T.K., Merdith, A.S., Rohling, E.J., Palmer, M.R., Foster, G.L., Bataille, C.P., Müller, R.D., 2021. Global chemical weathering dominated by continental arcs since the mid-Paleozoic. *Nat. Geosci.* 14, 690–696.

Goddéris, Y., Donnadieu, Y., Nedelec, A., Dupré, B., Dessert, C., Grard, A., Ramstein, G., François, L.M., 2003. The Sturtian 'snowball' glaciation. *Earth Plan. Sci. Lett.* 211, 1–12.

Goddéris, Y., Donnadieu, Y., Tombozafy, M., Dessert, C., 2008. Shield effect on continental weathering: Implication for climatic evolution of the Earth at the geological timescale. *Geoderma* 145, 439–448.

Goudie, A.S., Viles, H.A., 2012. Weathering and the global carbon cycle: Geomorphological perspectives. *Earth-Sci. Rev.* 113, 59–71.

Graly, J.A., Licht, K.J., Bader, N.A., Bish, D.L., 2020. Chemical weathering signatures from Mt. Achernar Moraine, Central Transantarctic Mountains I: Subglacial sediments compared with underlying rock. *Geochim. Cosmochim. Acta* 283, 149–166.

Guilbranson, E.L., Montañez, I.P., Tabor, N.J., Oscar Limarino, C., 2015. Late Pennsylvanian aridification on the southwestern margin of Gondwana (Paganica Basin, NW Argentina): A regional expression of a global climate perturbation. *Palaeogeogr. Palaeoclimatol. Palaeoecol.* 417, 220–235.

Guilbranson, E.L., Sheldon, N.D., Montañez, I.P., Tabor, N.J., McIntosh, J.A., 2022. Late Permian soil-forming paleoenvironments on Gondwana: A review. *Palaeogeogr., Palaeoclim., Palaeoecol.* 586, 110762.

Gurnell, A., 2013. Plants and river system engineers. *Earth Surf. Process. Landforms* 39, 4–25.

Halverson, G.P., Hurtgen, M.T., Porter, S.M., Collins, A.S., 2009. Neoproterozoic-Cambrian biogeochemical evolution. In: *Developments in Precambrian Geology*, vol. 16, pp. 351–365.

Hao, J., Sverjensky, D.A., Hazen, R.M., 2017. A model for late Archean chemical weathering and world average river water. *Earth Plan. Sci. Lett.* 457, 191–203.

Hao, J., Knoll, A.H., Huang, F., Hazen, R.M., Daniel, I., 2020. Cycling phosphorus on the Archean Earth: Part I. Continental weathering and riverine transport of phosphorus. *Geochim. Cosmochim. Acta* 273, 70–84.

Hartmann, J., Moosdorf, N., Lauerwald, R., Hinderer, M., West, A.J., 2014. Global chemical weathering and associated P-release – The role of lithology, temperature and soil properties. *Chem. Geol.* 363, 145–163.

Hausrath, E.M., Neaman, A., Brantley, S.L., 2009. Elemental release rates from dissolving basalt and granite with and without organic ligands. *Am. J. Sci.* 309, 633–660.

Hazen, R.M., Papineau, D., Bleeker, W., Downs, R.T., Ferry, J.M., McCoy, T.J., Sverjensky, D.A., Yang, H., 2008. Mineral evolution. *Am. Mineral.* 93, 1693–1720.

Heimsath, A.M., Burke, B.C., 2013. The impact of local geochemical variability on quantifying hillslope soil production and chemical weathering. *Geomorphology* 200, 75–88.

Hessler, A.M., Zhang, J., Vocault, J., Ambrose, W., 2017. Continental weathering coupled to Paleogene climate changes in North America. *Geology* 45, 911–914.

Hewawasam, T., von Blanckenburg, F., Bouchez, J., Dixon, J.L., Schüssler, J.A., Maekeler, R., 2013. Slow advance of the weathering front during deep, supply-limited saprolite formation in the tropical Highlands of Sri Lanka. *Geochim. Cosmochim. Acta* 118, 202–230.

Hintze, J.L., Nelson, R.D., 1998. Violin plots: A box plot-density trace synergism. *Am. Statistician* 52, 181–184.

Horodyskyj, L.B., White, T.S., Kump, L.R., 2012. Substantial biologically mediated phosphorus depletion from the surface of a Middle Cambrian paleosol. *Geology* 40, 503–506.

Husson, J.M., Peters, S.E., 2017. Atmospheric oxygenation driven by unsteady growth of the continental sedimentary reservoir. *Earth Plan. Sci. Lett.* 460, 68–75.

Hyland, E.G., Sheldon, N.D., 2016. Examining the spatial consistency of paleosol proxies: Implications for palaeoclimatic and palaeoenvironmental reconstructions in terrestrial sedimentary basins. *Sedimentology* 63, 959–971.

Hyland, E.G., Sheldon, N.D., Cotton, J.M., 2017. Constraining the early Eocene climatic optimum: A terrestrial interhemispheric comparison. *Bull. Geol. Soc. Am.* 129, 244–252.

Ielpi, A., Lapôtre, M.G.A., Gibling, M.R., Boyce, C.K., 2022. The impact of vegetation on meandering rivers. *Nat. Rev. Earth Env.* 3, 165–178.

Jenny, H., 1941. *Factors in Soil Formation*. McGraw-Hill, New York.

Jenny, H., Amundson, R., 1994. *Factors of Soil Formation: A System of Quantitative Pedology*.

Jobbagy, E.G., Jackson, R.B., 2001. The distribution of soil nutrients with depth: Global patterns and the imprint of plants. *Biogeochem.* 53, 51–77.

Jolivet, M., Boulvais, P., 2021. Global significance of oxygen and carbon isotope compositions of pedogenic carbonates since the Cretaceous. *Geosci. Front.* 12. <https://doi.org/10.1016/j.gsf.2020.12.012>.

Kahmann, J.A., Seaman III, J., Driese, S.G., 2008. Evaluating Trace Elements as Paleoclimate Indicators: Multivariate Statistical Analysis of Late Mississippian Pennington Formation Paleosols, Kentucky, U.S.A. *J. Geol.* 116, 254–268.

Kanzaki, Y., Murakami, T., 2015. Estimates of atmospheric CO<sub>2</sub> in the Neoproterozoic from paleosols. *Geochim. Cosmochim. Acta* 159, 190–219.

Kasting, J.F., 1993. Earth's Early Atmosphere. *Science* 259, 920–926.

Kelly, D.C., Zachos, J.C., Bralower, T.J., Schellenberg, S.A., 2005. Enhanced terrestrial weathering/runoff and surface ocean carbonate production during the recovery stages of the Paleocene–Eocene thermal maximum. *Paleoceanography* 20, 1–11.

Kendall, B., Creaser, R.A., Reinhard, C.T., Lyons, T.W., Anbar, A.D., 2015. Transient episodes of mild environmental oxygenation and oxidative continental weathering during the late Archean. *Sci. Adv.* 1, e1500777.

Kennedy, M.J., Droser, M., Mayer, L.M., Pevear, D., Mrofka, D., 2006. Late Precambrian Oxygenation: Inception of the Clay Mineral Factory. *Science* 311, 1446–1450.

Kidston, R., Lang, W.H., 1921. On Old Red Sandstone plants showing structure from the Rhynie Chert bed, Aberdeenshire. Part V. The Thallophyta occurring in the peat bed, the succession of plants through a vertical section of the bed and the conditions of accumulation. *R. Soc. Edinburgh Trans.* 52, 855–902.

Korenaga, J., 2018. Crustal evolution and mantle dynamics through Earth history. *Phil. Trans. R. Soc. A Math. Phys. Eng. Sci.* 376, 20170408.

Krasilov, V.A., 1981. Orestovia and the origin of vascular plants. *Lethaia* 14, 235–250.

Kraus, M.J., 1999. Paleosols in clastic sedimentary rocks: their geologic applications. *Earth-Sci. Rev.* 47, 41–70.

Kraus, M.J., Riggins, S., 2007. Transient drying during the Paleocene–Eocene Thermal Maximum (PETM): Analysis of paleosols in the bighorn basin, Wyoming. *Palaeogeogr. Palaeoclim. Palaeoecol.* 245, 444–461.

Laakso, T.A., Sperling, E.A., Johnston, D.T., Knoll, A.H., 2020. Ediacaran reorganization of the marine phosphorus cycle. *Proc. Natl. Acad. Sci.* 117, 11961–11967.

Lee, C.T.A., Thurner, S., Paterson, S., Cao, W., 2015. The rise and fall of continental arcs: Interplays between magmatism, uplift, weathering, and climate. *Earth Plan. Sci. Lett.* 425, 105–119.

Lenton, T.M., 2001. The role of land plants, phosphorus weathering and fire in the rise and regulation of atmospheric oxygen. *Glob. Chang. Biol.* 7, 613–629.

Lenton, T.M., Watson, A.J., 2004. Biotic enhancement of weathering, atmospheric oxygen and carbon dioxide in the Neoproterozoic. *Geophys. Res. Lett.* 31.

Liivamägi, S., Somelar, P., Vircava, I., Mahaney, W.C., Kirs, J., Kirsimäe, K., 2015. Petrology, mineralogy and geochemical climofunctions of the Neoproterozoic Baltic paleosol. *Precambrian Research* 256, 170–188. <https://doi.org/10.1016/j.precamres.2014.11.008>.

Lipp, A.G., Shortle, O., Sperling, E.A., Brocks, J.J., Cole, D., Crockford, P.W., Del Mouro, L., Dewing, K., Dornbos, S.Q., Emmings, J.F., Farrell, U.C., Jarrett, A., Johnsons, B. W., Kabanov, P., Keller, C.B., Kunzmann, M., Miller, A.J., Mills, N.T., O'Connell, B., Peters, S.E., Planavsky, N.J., Ritter, S.R., Schoepfer, S.D., Wilby, P.R., Yang, J., 2021. The composition and weathering of the continents over geologic time. *Geochim. Perspect. Lett.* 17, 21–26.

Longman, J., Mills, B.J.W., Manners, H.R., Gernon, T.M., Palmer, M.R., 2021. Late Ordovician climate change and extinctions driven by elevated volcanic nutrient supply. *Nat. Geosci.* 14, 924–929.

Longman, J., Mills, B.J.W., Donnadieu, Y., Goddérus, Y., 2022. Assessing volcanic controls on Miocene climate change. *Geophys. Res. Lett.* 49, e2021GL096519.

Lucas, Y., 2001. The role of plants in controlling rates and products of weathering: Importance of biological pumping. *Ann. Rev. Earth Plan. Sci.* 29, 135–163.

Lyons, T.W., Reinhard, C.T., Planavsky, N.J., 2014. The rise of oxygen in Earth's early ocean and atmosphere. *Nature* 506, 307–315.

Macdonald, F.A., Swanson-Hysell, N.L., Park, Y., Lisiecki, L., Jagoutz, O., 2019. Arc-continent collisions in the tropics set Earth's climate state. *Science* 364, 181–184.

Malone, D.H., Stein, C.A., Craddock, J.P., Kley, J., Stein, S., Malone, J.E., 2016. Maximum depositional age of the Neoproterozoic Jacobsville Sandstone, Michigan: Implications for the evolution of the Midcontinent Rift. *Geosphere* 12, 1271–1282.

Markewich, H.W., Pavich, M.J., Buell, G.R., 1990. Contrasting soils and landscapes of the Piedmont and Coastal Plain, eastern United States. *Geomorphology* 3, 417–447.

Martin, E.E., Macdougall, J.D., 1995. Sr and Nd isotopes at the Permian/Triassic boundary: A record of climate change. *Chem. Geol.* 125, 73–99.

Martin, J.B., Pain, A.J., Martin, E.E., Rahman, S., Ackerman, P., 2020. Comparisons of nutrients exported from Greenlandic glacial and deglaciated watersheds. *Geobiology* 18, e2020GB006661.

Maynard, J.B., 1992. Chemistry of modern soils as a guide to interpreting Precambrian paleosols. *J. Geol.* 100, 279–289.

Meyers, S.R., Peters, S.E., 2011. A 56 million year rhythm in North American sedimentation during the Phanerozoic. *Earth Plan. Sci. Lett.* 303, 174–180.

Michel, L.A., Sheldon, N.D., Myers, T.S., Tabor, N.J., 2022. Assessment of pretreatment methods on CIA-K and CALMAG indices and the effects of paleoprecipitation estimates. *Palaeogeogr. Palaeoclim. Palaeoecol.* (accepted).

Millot, R., Gaillardet, J., Dupré, B., Allègre, C.J., 2002. The global control of silicate weathering rates and the coupling with physical erosion: New insights from rivers of the Canadian Shield. *Earth Plan. Sci. Lett.* 196, 83–98.

Mills, B.J.W., Watson, A.J., Goldblatt, C., Boyle, R., Lenton, T.M., 2011. Timing of Neoproterozoic glaciations linked to transport-limited global weathering. *Nat. Geosci.* 4, 861–864.

Modenesi-Gauttieri, M.C., de Toledo, M.C.M., Hiruma, S.T., Taioli, F., Shimada, H., 2011. Deep weathering and landscape evolution in a tropical plateau. *Catena* 85, 221–230.

Molnar, P., England, M.H., 1990. Late Cenozoic uplift of mountain ranges and climate: chicken or egg? *Nature* 346, 29–34.

Morris, J.L., Leake, J.R., Stein, W.E., Berry, C.M., Marshall, J.E., Wellman, C.H., Milton, J. A., Hillier, S., Mannolini, F., Quick, J., Beerling, D.J., 2015. Investigating Devonian trees as geo-engineers of past climates: Linking paleosols to palaeobotany and experimental geobiology. *Palaeontology* 58, 787–801.

Murakami, T., Ito, J.I., Utsunomiya, S., Kasama, T., Kozai, N., Ohnuki, T., 2004. Anoxic dissolution processes of biotite: Implications for Fe behavior during Archean weathering. *Earth Plan. Sci. Lett.* 224, 117–129.

Neaman, A., Chorover, J., Brantley, S.L., 2005. Implications of the evolution of organic acid moieties for basalt weathering over geological time. *Am. J. Sci.* 305, 147–185.

Nesbitt, H.W., Young, G.M., 1982. Early Proterozoic climates and plate motions inferred from major element chemistry of lutites. *Nature* 299, 715–717.

Norton, K.P., Molnar, P., Schlunegger, F., 2014. The role of climate-driven chemical weathering on soil production. *Geomorphology* 204, 510–517.

Nott, J., 1994. The influence of deep weathering on coastal landscape and landform development in the monsoonal tropics of Northern Australia. *J. Geol.* 102, 509–522.

Och, L.M., Shields-Zhou, G.A., 2012. The Neoproterozoic oxygenation event: Environmental perturbations and biogeochemical cycling. *Earth-Sci. Rev.* 110, 26–57.

Olesen, O., Kierulf, H.P., Brönnér, M., Dalsegg, E., Fredin, O., Solbakk, T., 2013. Deep weathering, neotectonics and strandflat formation in Nordland, northern Norway. *Nor. Geol. Tidsskr.* 93, 189–213.

Park, Y., Maffre, P., Goddérus, Y., Macdonald, F.A., Anttila, E.S.C., Swanson-Hysell, N. L., 2020. Emergence of the Southeast Asian islands as a driver for Neogene cooling. *Proc. Nat. Acad. Sci. U.S.A.* 117, 25319–25326.

Pastor-Galán, D., Nance, R.D., Murphy, J.B., Spencer, C.J., 2019. Supercontinents: Myths, mysteries, and milestones. *Geol. Soc. Spec. Publ.* 470, 39–64.

Pawlak, L., Buma, B., Šamonil, P., Kvaček, J., Gałazka, A., Kohout, P., Malik, I., 2020. Impact of trees and forests on the Devonian landscape and weathering processes with implications to the global Earth's system properties – A critical review. *Earth-Sci. Rev.* 205, 103200.

Peters, S.E., Husson, J.M., 2017. Sediment cycling on continental and oceanic crust. *Geology* 45, 323–326.

Peters, S.E., Husson, J.M., Czaplewski, J.M., 2018. A platform for geological data integration and deep-time Earth crust research. *Geochem., Geophys., Geosys.* 19, 1393–1409.

Phillips, J.D., 2010. The convenient fiction of steady-state soil thickness. *Geoderma* 156, 389–398.

Planavsky, N.J., Rouzel, O.J., Bekker, A., Lalonde, S.V., Konhauser, K.O., Reinhard, C.T., Lyons, T.W., 2010. The evolution of the marine phosphate reservoir. *Nature* 467, 1088–1090.

Planavsky, N.J., Cole, D.B., Ison, T.T., Reinhard, C.T., Crockford, P.W., Sheldon, N.D., Lyons, T.W., 2018. A case for low atmospheric oxygen levels during Earth's middle history. *Emerg. Top. Life Sci.* 2, 149–159.

Porada, P., Lenton, T.M., Pohhl, A., Weber, B., Mander, L., Donnadieu, Y., Beer, C., Poschl, U., Kleidon, A., 2016. High potential for weathering and climate effects of non-vascular vegetation in the Late Ordovician. *Nat. Commun.* 7, 12113.

Prochnov, S.J., Nordt, L.C., Atchley, S.C., Hudec, M.R., 2006. Multi-proxy paleosol evidence for middle and late Triassic climate trends in eastern Utah. *Palaeogeogr. Palaeoclimatol. Palaeoecol.* 232, 53–72.

Ramos, E.J., Breecker, D.O., Barnes, J.D., Li, F., Gingerich, P.D., Loewy, S.L., Satkoski, A. M., Baczyński, A.A., Wing, S.L., Miller, N.R., Lassiter, J.C., 2022. Swift weathering response on floodplains during the Paleocene–Eocene Thermal Maximum. *Geophys. Res. Lett.* 49, e2021GL097436.

Raymo, M.E., Ruddiman, W.F., 1992. Tectonic forcing of late Cenozoic climate. *Nature* 359, 117–122.

Regmi, A.D., Yoshida, K., Dhital, M.R., Pradhan, B., 2014. Weathering and mineralogical variation in gneissic rocks and their effect in Sangrumba Landslide, East Nepal. *Environ. Earth Sci.* 71, 2711–2727.

Reinhard, C.T., Raiswell, R., Scott, C., Anbar, A.D., Lyons, T.W., 2009. A Late Archean Sulfidic Sea Stimulated by Early Oxidative Weathering of the Continents. *Science* 326, 713–716.

Reinhard, C.T., Planavsky, N.J., Gill, B.C., Ozaki, K., Robbins, L.J., Lyons, T.W., Fischer, W.W., Wang, C., Cole, D.B., Konhauser, K.O., 2017. Evolution of the global phosphorus cycle. *Nature* 541, 386–389.

Reinhard, C.T., Planavsky, N.J., Ward, B.A., Loce, G.D., Le Hir, G., Ridgwell, A., 2020. The impact of marine nutrient abundance on early eukaryotic ecosystems. *Geobiology* 18, 139–151.

Retallack, G.J., 2001. Soils of the Past: An Introduction to Paleopedology. Oxford, United Kingdom.

Retallack, G.J., Vevers, J.J., Morante, R., 1996. Global coal gap between Permian–Triassic extinction and Middle Triassic recovery of peat-forming plants. *GSA Bulletin* 108, 195–207.

Retallack, G.J., 2012. Criteria for distinguishing microbial mats and earths. In: *Microbial Mats in Siliciclastic Depositional Systems Through Time* 139–152. SEPM Society for Sedimentary Geology.

Rudnick, R.L., Gao, S., 2003. In: Rudnick, R.L. (Ed.), *The Crust, Treatise in Geochemistry*, vol. 3, Elsevier, Amsterdam, pp. 1–64.

Rye, R., Holland, H.D., 1998. Paleosols and the evolution of atmospheric oxygen: a critical review. *Am. J. Sci.* 298, 621–672.

Rye, R., Holland, H.D., 2000. Life associated with a 2.76 Ga ephemeral pond?: Evidence from Mount Roe #2 paleosol. *Geology* 28, 483–486.

Sadler, P.M., Bruns, P., Haas, H.C., 1999. The Influence of Hiatuses on Sediment Accumulation Rates On the Determination of Sediment Accumulation Rates. *GeoRes. Forum* 5, 15–40.

Sahoo, S.K., Planavsky, N.J., Kendall, B., Wang, X., Shi, X., Scott, C., Anbar, A.D., Lyons, T.W., Jiang, G., 2012. Ocean oxygenation in the wake of the Marinoan glaciation. *Nature* 489, 546–549.

Sayyed, M.R.G., 2014. Flood basalt hosted palaeosols: Potential palaeoclimatic indicators of global climate change. *Geosci. Front.* 5, 791–799.

Schaller, M.F., Wright, J.D., Kent, D.V., 2011. Atmospheric  $p\text{CO}_2$  Perturbations Associated with the Central Atlantic Magmatic Province. *Science* 331, 1404–1410.

Schaller, M.F., Wright, J.D., Kent, D.V., 2014. A 30 Myr record of late Triassic atmospheric  $p\text{CO}_2$  variation reflects a fundamental control of the carbon cycle by changes in continental weathering. *Bull. Geol. Soc. Am.* 127, 661–671.

Schumer, R., Jerolmack, D.J., 2009. Real and apparent changes in sediment deposition rates through time. *J. Geophys. Res.: Earth Surf.* 114, F00A06.

Sheldon, N.D., 2006a. Precambrian paleosols and atmospheric  $\text{CO}_2$  levels. *Precam. Res.* 147, 148–155.

Sheldon, N.D., 2006b. Using paleosols of the Picture Gorge Basalt to reconstruct the middle Miocene climatic optimum. *Paleobios* 26, 27–36.

Sheldon, N.D., 2006c. Abrupt chemical weathering increase across the Permian-Triassic boundary. *Palaeogeogr. Palaeoclim. Palaeoecol.* 231, 315–321.

Sheldon, N.D., Retallack, G.J., Tanaka, S., 2002. Geochemical Climofunctions from North American Soils and Application to Paleosols across the Eocene-Oligocene Boundary in Oregon. *J. Geol.* 110, 687–696.

Sheldon, N.D., Tabor, N.J., 2009. Quantitative paleoenvironmental and paleoclimatic reconstruction using paleosols. *Earth-Sci. Rev.* 95, 1–52.

Sheldon, N.D., Costa, E., Cabrera, L., Garcés, M., 2012. Continental climatic and weathering response to the Eocene-Oligocene transition. *J. Geol.* 120, 227–236.

Sheldon, N.D., 2013. Causes and consequences of low atmospheric  $\text{CO}_2$  in the Late Mesoproterozoic. *Chem. Geol.* 362, 224–231.

Sheldon, N.D., Mitchell, R.L., Dzombak, R.M., 2021. Reconstructing Precambrian  $p\text{CO}_2$  and  $p\text{O}_2$  Using Paleosols. Cambridge University Press.

Smith, D.E., Zuber, M.T., Solomon, S.C., Phillips, R.J., Head, J.W., Garvin, J.B., Banerdt, W.B., Muhleman, D.O., Pettengil, G.H., Neumann, G.A., Lemoine, F.G., Abshire, J.B., Aharonson, O., David, C., Brown, Hauck, S.A., Ivanov, A.B., McGovern, P.J., Zwally, H.J., Duxbury, T.C., 1999. The global topography of Mars and implications for surface evolution. *Science* 284, 1495–1503.

Somelar, P., Soomer, S., Driese, S.G., Lepland, A., Stinchcomb, G.E., Kirsimae, K., 2020.  $\text{CO}_2$  drawdown and cooling at the onset of the Great Oxidation Event recorded in 2.45 Ga paleoweathering crust. *Chem. Geol.* 548, 119678.

Sternai, P., Caricchi, L., Pasqueri, C., Garzanti, E., van Hinsbergen, D.J.J., Castelltort, S., 2019. Magmatic forcing of Cenozoic climate? e2018JB016460 *J. Geophys. Res. Solid Earth* 125. <https://doi.org/10.1029/2018JB016460>.

Stockmann, U., Minasny, B., McBratney, A.B., 2014. How fast does soil grow? *Geoderma* 216, 48–61.

Tabor, N.J., Montañez, I.P., Scotese, C.R., Poulsen, C.J., Mack, G.H., 2008. Paleosol archives of environmental and climatic history in paleotropical western Pangea during the latest Pennsylvanian through Early Permian. *Geol. Soc. Am. Spec. Pap.* 2441, 291–303.

Taylor, S.R., McLennan, S.M., 1985. The Continental Crust: Its Composition and Evolution. Blackwell, United States.

Taylor, S.R., McLennan, S.M., 1995. The geochemical evolution of the continental crust. *Rev. Geophys.* 33, 241–265.

Theiling, B.P., Elrick, M., Asmerom, Y., 2012. Increased continental weathering flux during orbital-scale sea-level highstands: Evidence from Nd and O isotope trends in Middle Pennsylvanian cyclic carbonates. *Palaeogeogr. Palaeoclim. Palaeoecol.* 342–343, 17–26.

USDA-NRCS, 2005. Soil Map of the World, Digitized by ESRI. Soil Climate Map, Soil Science Division, World Soil Resources, Washington, D.C. Accessible online at: [https://www.nrcs.usda.gov/wps/portal/nrcs/detail/soils/use/?cid=nrcs142p2\\_054013](https://www.nrcs.usda.gov/wps/portal/nrcs/detail/soils/use/?cid=nrcs142p2_054013).

van de Schootbrugge, B. et al., 2020. Catastrophic soil loss associated with end-Triassic deforestation. *Earth-Science Rev.* 210, 103332.

Von Strandmann, P.A.E., Jones, M.T., West, A.J., Murphy, M.J., Stokke, E.W., Tarbuck, G., Wilson, D.J., Pearce, C.R., Schmidt, D.N., 2021. Lithium isotope evidence for enhanced weathering and erosion during the Paleocene-Eocene Thermal Maximum. *Sci. Adv.* 7, eabh4224. <https://doi.org/10.1126/sciadv.abh4224>.

Wang, W., Cawood, P.A., Spencer, C.J., Pandit, M.K., Zhao, J.H., Xia, X.P., Zheng, J.P., Lu, G.M., 2021. Global-scale emergence of continental crust during the Mesoproterozoic-early Neoarchean. *Geology*. <https://doi.org/10.1130/G49418.1>.

Wellman, C.H., Strother, P.K., 2015. The terrestrial biota prior to the origin of land plants (embryophytes): A review of the evidence. *Palaeontology* 58, 601–627.

West, A.J., 2012. Thickness of the chemical weathering zone and implications for erosional and climatic drivers of weathering and for carbon-cycle feedbacks. *Geology* 40, 811–814.

Willenbring, J.K., Von Blanckenburg, F., 2010. Long-term stability of global erosion rates and weathering during late-Cenozoic cooling. *Nature* 465, 211–214.



**Rebecca Dzombak** received her B.S. in 2015 and Ph.D. in 2021 from the Department of Earth and Environmental Sciences at the University of Michigan. Her dissertation focused on constraining baselines and evolutions in terrestrial geochemistry, with a focus on weathering and biologically relevant elements (P, Fe).



**Nathan Sheldon** is a Professor at the University of Michigan. He received his B.A. (1999) from Carleton College and Ph.D. (2003) from the University of Oregon. His research interests include paleoclimatology, geobiology, and global change biology and he has published nearly 100 papers in those fields. He is a Fellow of the Geological Society of America (GSA) and of the American Association for the Advancement of Science (AAAS), and received the James Lee Wilson Medal from SEPM.